JOURNAL OF MATERIALS SCIENCE 22 (1987) 278–300

Conversion of acrylonitrile-based precursor fibres to carbon fibres

Part 1 *A review of the physical and morphological aspects*

MUKESH K. JAIN*, A. S. ABHIRAMAN‡
Georgia Institute of Technology, Atlanta, Georgia 30332, USA

The physical and morphological aspects of the conversion of acrylonitrile-based precursors to carbon fibres are reviewed. The development of structure through the different stages of the process, namely precursor fibre formation, oxidative stabilization and carbonization, is described. The interactive contributions of process conditions and the precursor structures to the morphology and the properties of carbon fibres are discussed.

1. Introduction

Carbon or graphite fibre composites are emerging as important construction materials in applications where light weight and high strength and modulus are the prime requirements. Basal planes of graphite crystal possess enormous mechanical strength but the resistance to shear between the planes is poor, causing most ordinary carbons and graphites to exhibit low stiffness and strength. A possible solution to this problem was discovered in one-dimensional form whereby the strong bonds are preferentially oriented along the axis of a whisker or fibre. Experimental whiskers produced in the laboratory [1, 2] have displayed excellent properties close to the theoretical limits of crystal properties, but it has not been possible to develop an industrially useful process for their production. The line of attack that has yielded results of more practical value is through the carbonization of fibres such as rayon, pitch and acrylic fibres.

Although large quantities of carbon fibre and cloth made from cellulose-based precursors are produced for various industrial applications, generally their mechanical properties are poor. Improvements in the mechanical properties of rayon-based carbon fibres are possible by stretching such fibres during high-temperature carbonization [3, 4]. Nevertheless, the hot-stretching process remains intrinsically difficult and expensive and appropriate precursor materials are no longer commercially produced to the extent necessary. Shindo of Japan [5–8] discovered about 20 years ago that carbonization of air-oxidized polyacrylonitrile (PAN) fibre produces a material with appreciable crystalline orientation. Later, British investigators discovered that if PAN fibres were suitably stressed during a carefully controlled process of oxidative stabilization, the resultant fibres obtained after carbonization using temperatures in excess of 1000° C were highly oriented and possessed good tensile strength and modulus [9]. Since then, a great deal of work had been published on the production, structure and physical properties of these fibres. There have been several excellent reviews [10–16] and doctoral theses [17–24] dealing with the study of PAN-based carbon fibres. The industrial efforts have been to produce a consistently high performance product at low cost. The approaches to this include modifications, chemical as well as physical, of the precursor and new innovative methods for stabilization and carbonization. Advances in the technology of the fibre manufacturing process have made it possible to produce carbon fibres with improved quality at much lower cost. Mesophase pitch is the latest raw material for producing high strength and high modulus carbon fibres (up to 120×10^6 psi modulus, $\sim 8.27 \times 10^5\,\mathrm{N\,mm^{-2}}$) without high-temperature stretching. In this report, however, the discussion will be confined to PAN-based carbon fibres.

2. Carbon fibre manufacturing processes

The manufacture of carbon fibres from PAN-based precursors, as disclosed in various patents, consists of a low-temperature oxidative stabilization in air followed by a high-temperature carbonization in an inert atmosphere. The PAN copolymer used for spinning precursor fibres usually contains about 2 to 10% of a comonomer such as methyl acrylate (MA) or methyl methacrylate (MMA). A small amount of a third comonomer which initiates the stabilization reactions at lower temperatures is often present in the precursor fibres. Both dry and wet spinning techniques using organic solvents such as dimethyl formamide (DMF) and sodium thiocyanate have been employed for spinning precursor fibres. In some instances, use of inorganic solvents involving ionic salts is found to have a detrimental effect on the thermal stability of the carbon fibres [25, 26]. PAN fibres spun by a melt spinning process have been developed recently by American Cyanamid Co. [27], which are also being explored for carbon fibre production. Fine filaments,

---

*Present address: ALCAN, Arvida Laboratories and Experimental Engineering Center, Jonquiere, Quebec, Canada.
‡Author to whom all correspondence should be addressed.

0022–2461/87 $03.00 + .12

usually 1 to 3 denier/filament, are employed in the form of a continuous tow containing 100 to 50 000 filaments for carbon fibre manufacture. The preoxidation or stabilization of these tows is carried out at 200 to 300° C for sufficient time to render them infusible and flameproof. Temperatures below about 200° C are impractical since very long periods are required, while temperatures above about 300° C cause violent exothermic reactions [28, 29] resulting in significant weight loss [30] and formation of tarry substances. Oxidative stabilization is very critical to the production of carbon fibres. Improper stabilization could result in blow out of a core portion during carbonization [31, 32] due to its incomplete oxidation. Proper conditions of rate of heating and time and temperature of heating should, therefore, be established for optimum stabilization for each precursor. In a batch process, heating the precursor in air at 220 to 250° C was employed by early workers, whereas modern practice is to pass the precursor tow continuously through a furnace divided into several zones with increasing temperature profiles. A residence time of several hours is usually required for complete stabilization [33–35], which is generally carried out in air but oxygen or oxidizing gases may be substituted for air [36–39]. The density of precursor fibre increases continuously while the white precursor changes to a shiny black fibre.

In spite of several studies using various analytical tools such as infrared spectroscopy [39–54], thermal analysis [55–64], gas chromatography [57, 64, 65–69], mass spectroscopy [34, 66, 70, 71] and wet chemical techniques [56, 72, 73], the chemistry of stabilization remains complicated and not well understood. The cyclization of nitrile pendant groups of PAN to give polyimine type structure seems to be well accepted as the main reaction during stabilization [30, 70, 74]. These imine sequences are postulated to be three to six units long. The effect of various comonomers in initiating or terminating the cyclization reactions has been studied in detail by Grassie and his colleagues [75–82] using thermal techniques. Some weight loss from chain scission and elimination of hydrogen cyanide and ammonia accompanies the cyclization reactions [34, 55, 83, 84]. Oxygen, which is added during stabilization, is mostly present as –OH and >CO groups [41, 55, 84–87] but some authors, based on infrared spectroscopic and model compound studies, have suggested that oxygen becomes attached to the imine nitrogen atoms to give a nitrone (>N–O) moiety [74, 85–89]. The presence of oxygen promotes cross-linking and is also believed to help in the aromatization of the cyclized sequences by the elmination of water, both being essential for the basal plane formation in carbon fibres. Various mechanisms of thermo-oxidative degradation of PAN polymer have been reviewed by Peebles [90].

The application of tension during the oxidation of precursor fibre is important since it prevents polymer chains from relaxing and losing their orientation, which becomes locked-in through cross-linking. Both physical and chemical [91, 92] changes during stabilization are affected by the presence of tension. The stabilized fibres show an amorphous X-ray pattern, but a high degree of crystalline order and orientation is displayed after their carbonization at temperatures in excess of 2000° C. A detailed discussion of morphological changes in precursor fibre as it undergoes stabilization and carbonization will be given in a later section. The extent of shrinkage or extension allowed during stabilization varies over a wide range depending on the precursor and the manufacturing process. A patent by Johnson *et al.* [9] allows a shrinkage of less than 12% whereas a 40 to 70% shrinkage of Beslon fibres has been suggested in a patent by Toho Beslon Co. [93]. A patent by NRDC [94] allows no shrinkage. Yet another patent by Japan Exlan Co. [95] recommends 0 to 50% extension during stabilization. The influence of various tensions and corresponding length changes during stabilization on the mechanical properties of carbon fibres will be discussed in a separate section.

Various measurements have been suggested for the optimization of conditions for oxidative stabilization. One which is more popular is the measurement of oxygen content as a function of stabilization time or temperature [33, 86, 91, 92, 96–103]. A stabilized fibre is considered suitably stabilized when its oxygen content is in the range of 8 to 12% [93]. An oxygen content of more than 12% results in the deterioration of stabilized fibre quality which gives low-quality carbon fibre, whereas less than 8% oxygen results in low yield of carbon fibres due to excessive weight loss during carbonization [31].

Since stabilization is the speed-limiting step in the production of carbon fibres, variations from the conventional stabilization processes described above have been attempted to speed up this step. One approach has been to modify the chemical composition of the precursor fibre either by using a comonomer [43, 94, 104–106] or an additive [107], or by impregnation with chemicals [108–113], which enhance stabilization. A patent by Japan Exlan Co. [105] describes this approach by using precursor fibres (1.3 denier/filament) spun from a PAN copolymer containing 2% methacrylic acid. These fibres, when passed through a furnace having a temperature gradient from 200 to 280° C, required only 25 min for complete stabilization. A second approach has been to modify the stabilization conditions and apparatus to speed up stabilization. A recent patent by Great Lakes Corp. [114] uses a V-shaped temperature profile instead of the more popular ascending one for continuous stabilization. Precursor fibres are first heated to a temperature 2 to 8° C short of fusion followed by cooling at a predetermined rate until a critical density is reached and then heated again until a density greater than 1.35, capable of sustaining carbonization temperature of at least 800° C, is obtained. A typical stabilization time of 25 min has been reported. Another patent by Toray Industries [32] claims a 2 to 20 min stabilization time by contacting the precursor fibre with a heated surface in the presence of an oxidizing gas. Speeds over 20 m min^{-1} have been claimed making it possible to couple stabilization with precursor spinning. Yet another approach for speeding up the stabilization has been to use non-air environments [115–118].

The carbonization of preoxidized or stabilized fibres is caried out in an inert atmosphere containing gases such as nitrogen or argon. The temperature of carbonization is usually decided by the type of application of the resulting carbon fibres. For high-strength applications, heating at 1500 to 1600° C is preferred since above this temperature a decrease in the tensile strength has been observed [33, 119–121]. For preparing high modulus carbon fibres, an additional heat treatment at 2500 to 3000° C is required. Nitrogen cannot be used at temperatures above about 2000° C due to its reaction with carbon to form cyanogen. The rate of heating and residence time during carbonization vary depending on the type of precursor and stabilization conditions. There is a large weight loss (up to 50%) during this stage, producing a large volume of volatiles and some tarry substances. The heating rates, therefore, have to be carefully controlled to avoid fibre damage during the release of volatiles. The gases evolved during carbonization consist mainly of H_2O and CO_2 at 300 to 500° C from dehydrogenation and cross-linking [34, 70]. This is followed by the evolution of HCN and N_2 at temperatures higher than 600° C, mainly due to the intermolecular condensation of ladder-type structures (containing ring nitrogen) into large sections, known as basal planes [34, 70, 122]. Other pyrolysis products identified during carbonization are H_2, NH_3, CO, CH_4 and C_4 hydrocarbons [57, 70]. The relative fractions of these gases have been shown by Bromley [57] to vary with the rate of heating. The structure of stabilized fibre changes from essentially amorphous to partly crystalline after heat treatment temperature (HTT) in the 1200 to 1500° C range and highly crystalline after HTT of > 2500° C.

Relatively long times have been reported in early patents for carbonization whereas modern practice is to pass stabilized fibres through an increasing temperature profile giving a total residence time of only a few minutes. In a 1970 patent issued to Great Lakes Corp. [35], the oxidized yarn was placed in a kiln and its temperature was raised to 1000° C in 4 h. For high-modulus fibres, the temperature was further raised to 2500° C in about 90 min and was kept at that level for 30 min. A more recent patent [123], however, described two furnaces, a vertical furnace maintained at 500 to 1000° C and a transverse furnace maintained at 800 to 2000° C, through which preoxidized strands are passed at a rate of $25\,\mathrm{m\,h^{-1}}$. The furnaces had a length of 2 and 1.8 m, respectively, giving a total residence time of about 9 min. A process described by Ezekeil [124–127] for the preparation of high-modulus carbon fibres uses a short time (1 min) exposure of oxidized yarn directly to 2500 to 2900° C without going through 1200 to 1500° C carbonization. Many variations of conventional carbonization have been reported. Stretching of carbon fibres during the HTT of 2500 to 3000° C has been reported to result in improvement in mechanical properties of the fibre [3, 128, 129]. Other variations include heating by an electric current passing through the fibre where the yarn establishes a temperature of 1800 to 3000° C [130], application of vibrational energy to the fibres while they are held under tension (0.2 to 1.2 g/denier) during carbonization and carbonization under hydrogen [130] and in nitrogen diluted with about 5% acetylene [131]. Catalytic amounts of boron compounds used during carbonization have been reported to improve the mechanical properties of resulting carbon fibres [132]. Similarly, immersion of carbon fibres in liquid bromine followed by its removal with an inert gas was shown to result in an increase in the tensile strength of carbon fibres [133].

3. Shrinkage and shrinkage force during carbon fibre manufacture

In order to minimize the relaxation of molecular orientation during stabilization, the precursor fibres are longitudinally constrained. Two methods have been used widely for constraining the fibres. In one, the fibre is heat treated while constrained to constant length and in the other, the fibre is restrained by a constant force during heat treatment. In a continuous process the stabilization can be carried out by feeding and removing the fibres at the same speed from the heat-treatment zone. Although the same feed and take-up speeds are maintained, the fibres can undergo compensating local shrinkage and extension during this treatment. For stabilization of fibres under constant tension, weights are placed on the thread-line and the feed or take-up speed is adjusted so as to maintain the weight position. When the fibre is heated with both ends fixed, a certain amount of tension or shrinkage force is generated as a result of the tendency of the molecular chains to coil, the extent of which depends on the initial morphology of the precursor. This initial tension could relax even without allowance for any macroscopic shrinkage if the polymer chains are not part of a continuous network between the two fixed ends. When a constant load is applied during stabilization, the fibre could shrink if the applied load is less than the shrinkage force, extend if the load applied is greater than the shrinkage force or maintain the same length if the applied load balances exactly the shrinkage force generated. The response under both constant force and constant length conditions is complicated by the simultaneous occurrence of chemical reactions which can influence the mobility in the system and thus the shrinkage and shrinkage force.

Length changes during the heating of unspecified acrylic fibres at 220° C in air under a constant load have been reported by Watt and Johnson [134]. At low loads the fibres shrank while at higher loads the fibres initially stretched and then shrank. Fitzer and co-workers [135, 136] also observed the latter behaviour upon heating Dralon-T fibres under the highest permissible load short of actual rupture. Contrary to Watt and Johnson, who attribute the shrinkage to molecular relaxation, Fitzer and Heym suggest that the shrinkage, which follows the plastic flow due to tensile loading, is chemical in nature and is caused by dehydrogenation at the points of atacticity [137] and by intermolecular cyclization [135, 136]. The initially parallel chains rotate during cyclization to a position in which they form an angle of 120 degrees with each other causing macroscopic shrinkage in the precursor. According to them a shrinkage of 13 to about 33% could result, depending on the type of ladder sequences formed. Layden [138] observed a different response from that observed by Watt and Johnson and Fitzer and co-workers during annealing of homopolymer PAN fibres. When small loads were applied, the fibre as it was heated to 270° C shrank initially, then stretched and finally shrank again. At larger loads, the fibre either shrank first and then stretched or just stretched without shrinking, depending on the magnitude of the applied load, and finally broke. Bahl and colleagues [36, 139] have reported a cumulative shrinkage of 27% for unidentified copolymer fibres and 34% for homopolymer fibres at 215° C in an oxygen environment. This shrinkage decreased when load was applied, showing a similar response as observed by Layden. The cumulative shrinkage was shown by them to consist of an instant initial or primary shrinkage of 3 and 10%, respectively, for copolymer and homopolymer fibres, followed by a slow secondary shrinkage. The primary shrinkage was found to be independent of the temperature and the atmosphere, whereas the secondary shrinkage was influenced by the temperature and environment. Both groups believe that the initial shrinkage is due to physical relaxation and that the secondary shrinkage is a result of chemical reactions similar to those suggested by Fitzer and co-workers [135–137]. Studies relating free shrinkage with the rates of heating have been reported by Fitzer and Heine [140].

The tension generated in a homopolymer PAN fibre during its heating to 270° C while held under constant length had been described by Layden [138]. Considerable tension was generated during heating to about 150° C, but it fell rapidly between 150 and 250° C and then rose again at 270° C, before levelling off finally with time. Warner *et al.* [141], using four different precursor fibres, observed an initial instantaneous shrinkage force and a delayed secondary shrinkage force when fibres were heated under constant length. The initial shrinkage force or tension depended upon the precursor processing history whereas the secondary shrinkage force was found to be related to stabilization kinetics. The increase of secondary shrinkage force with heating time was found to be parabolic in the case where the stabilized fibre cross-section was characterized by a two-zone morphology and linear when the fibre changed colour uniformly over the entire cross-sectional area. It was possible to define a temperature range for each type (and denier) of fibre, with the secondary shrinkage force increasing linearly with time in the lower temperature range and parabolically in the higher temperature range. The rate of increase in secondary shrinkage force was found higher for fibres drawn to higher draw ratios (lower denier), showing a linear relationship with the inverse of the square root of denier of the fibre. When the precursor fibre was passed continuously through a furnace with a temperature gradient from 230 to 290° C, different local velocities were observed throughout the hot zone in spite of the same feed and take-up velocities. The fibre shrank first, causing an increase in its denier, then it drew and finally it shrank again. This behaviour has been explained with the help of a model of fibre response. An oriented semi-crystalline fibre, when subjected to a temperature gradient between the feed and take-up rolls rotating at the same speeds, will first decelerate in the vicinity of the glass transition temperature (T_g) owing to entropic recovery and then accelerate to compensate for the decrease in its velocity. Chemical reactions produce a secondary shrinkage requiring a compensating amount of additional draw which occurs at the region in the threadline where the fibre offers the least amount of resistance (i.e., in the unreacted acrylic material after entropic shrinkage and not in the stabilized material). Recent papers by Takaku *et al.* [142, 143], where they have reported contractive stresses at different temperatures, show behaviour similar to that observed by others [36, 138, 141] at short times, but at longer times the stress due to secondary shrinkage reaches a maximum and shows a decrease on further heating. The peak position shifted to shorter times at higher temperatures, disappearing completely when the temperatures employed were as high as 280 to 290° C.

During carbonization of fully stabilized fibres a small (4 to 6%) shrinkage is observed. A higher shrinkage is seen if the fibres are incompletely stabilized. The additional shrinkage due to the continuation of stabilization reactions can, however, be controlled by the application of suitable loads during carbonization. Bromley [57] has shown the effect of rate of heating during carbonization on the length changes under various loads. Pyrolysis (up to 1000° C) of oxidized Courtelle fibres by heating at the rate of 40° C $\min^{-1}$ resulted in shrinkage under low loads but in extension under high loads over the temperature range 300 to 500° C. On slower pyrolysis, i.e. by heating for 30 min at a given temperature before it was raised a further 30° C, only shrinkage was observed even under high loads. Manocha *et al.* [37] observed that understabilized 6% methyl acrylate copolymer fibres shrank about 12% during carbonization which was reduced to 5% when the time of oxidation was increased and to 2% by the application of load during carbonization. Whether the precursor was allowed to shrink or was stretched during preoxidation had no effect on carbonization shrinkage. However, the same authors have reported, in a later publication, a large dependence of carbonization shrinkage on the amount of shrinkage allowed during the preoxidation of Beslon fibres [139]. High shrinkage during oxidation resulted in low carbonization shrinkage but when shrinkage during oxidation was suppressed by the application of load, a large shrinkage was observed during carbonization.

4. Development of carbon fibre structure

4.1. Structure of PAN fibres

The literature contains several references [144–156] to X-ray diffraction studies of PAN but few definite conclusions have been reached as to the crystal structure of this polymer. Typical wide-angle X-ray diffraction (WAXD) photographs of oriented fibre display an

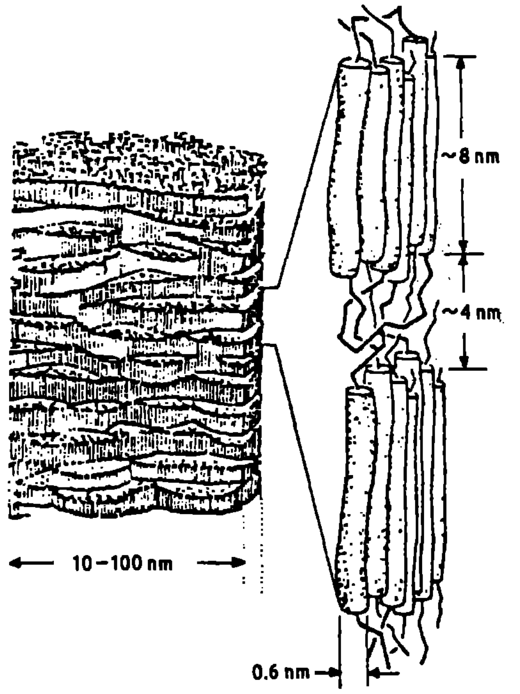

Figure 1 Morphological model of PAN fibre by Warner *et al.* [158], showing ordered and disordered regions.

intense and a faint arc at the equator which correspond to lattice spacings of approximately 0.52 and 0.3 nm, respectively [157, 158]. Off-equatorial reflections are usually absent, indicating the presence of only lateral order. Nevertheless, two types of unit cells, hexagonal [159] and orthorhombic [144, 148], have ben proposed by early workers. Holland *et al.* [154] were the first to grow single crystals of PAN, of plate-like texture, from a propylene carbonate solution. A stack of these gave only equatorial reflections on X-ray and electron diffraction [155]. The absence of off-equatorial reflections has been attributed by Lindenmeyer and Hosemann to the paracrystalline nature of these single crystals [146]. Recent X-ray studies by Kumamaru *et al.* [153] on single crystals grown during solution polymerization of acrylonitrile (AN) have, however, shown equatorial as well as meridional reflections. This three-dimensional order has also been reported in highly oriented films and fibres by others [144, 149, 160]. The unit cell proposed in some of the recent studies is orthorhombic, but different lattice parameters have been suggested by different researchers. A three-dimensional orthorhombic unit cell with $a = 2.148$, $b = 1.155$ and $c = 0.710\,\text{nm}$, has been proposed by Colvin and Storr [149] from their X-ray studies of PAN fibres. Based on this unit cell, the calculated crystalline density of PAN is $1.19\,\text{g}\,\text{cm}^{-3}$, which agrees quite well with the values quoted in the literature [161, 162].

Spherulites have been observed by Holland [163] and by Gohil *et al.* [164] in thin films of PAN, whereas fibres have been shown to possess a fibrillar structure. Precipitation of fibres from solution generates a spongy network which collapses and is drawn out during the stretching operation to produce a fibrillar morphology in PAN fibres [165]. Small-angle X-ray scattering studies reveal the presence of elongated

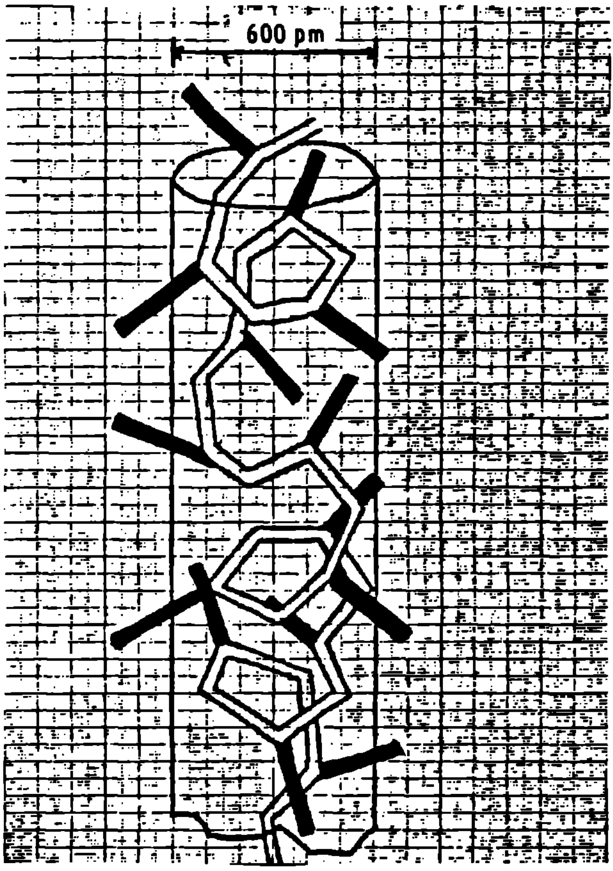

Figure 2 Irregular helix structure of PAN chains suggested by Olive and Olive [168].

micropores in these fibres. The fibrils, 10 to 100 nm diameter [166], and the micropores are aligned parallel to the fibre axis. A model proposed recently by Warner *et al.* [158] describes the fine structure within a typical fibril, where the ordered and disordered regions are connected along the fibre axis. The parallel rods constitute the major part of the ordered phase in a fibril. The rods are not in perfect alignment with respect to the rod ends, but rather exhibit some misalignment as depicted in Fig. 1. The disordered regions connecting the rods consist of loops, folds, entangled chains, defects, comonomer sequences, tie chains etc. The lateral dimensions of the ordered domains as estimated from WAXD data are in the range of 5 to 20 nm, depending on the thermal history of the precursor fibres. The length of these domains is of the other of 8 to 10 nm, roughly twice that of the disordered regions. The rod diameter is proposed to be approximately 0.6 nm based on WAXD [158, 167] and molecular model studies [158]. The large dipole moment of the nitrile groups, together with their close proximity in space, leads to very large intramolecular dipolar and steric repulsions which compel the individual macromolecules into a somewhat helical conformation [168]. As indicated in Fig. 2, the twisted, kinked molecule may be thought of as a more or less rigid structure, fitting within a cylinder, which is not appreciably deformed on drawing. The random orientation of nitrile groups in space in this model explains the observed low infrared dichroic ratios [156, 169, 170] and optical birefringence [156–170].

Commercial PAN precursor fibres are rarely pure but contain up to 10% comonomer. X-ray scattering peaks are broader [150, 151] and the extents of crystallization lower [150] in copolymers than in pure PAN. The accuracy of extents of crystallization as estimated from the area under the diffraction peak is, however, debatable in PAN polymer and fibres. Amorphous PAN polymer, prepared by using organometallic catalysts, gives rise to diffuse X-ray diffraction peaks [152] which overlap with the crystalline peaks, making the measurement of crystallinity highly unreliable in PAN polymer and fibres. The calculation of crystallinity using density measurements, frequently used in semi-crystalline polymers, fails in the case of PAN due to similar densities of the crystallized and uncrystallized samples [172, 173]. Differential scanning calorimetry (DSC) has often been used to estimate the extent of crystallization in semi-crystalline polymers from the area under the melting curve. This technique is also not suitable for PAN fibres due to their degradation before melting. A novel method has, however, been employed recently by Frushour [174, 175] where the melting behaviour of PAN copolymers is studied by DSC in a pressure cell containing water, which depresses the melting point of PAN by over 100° C [174], shifting it to well below the degradation temperature. This technique has been claimed to be very sensitive to even small differences in crystallinity. Even though absolute measurements of the extents of crystallization are still not possible, this technique may prove useful for relative measures of the extent of crystallization through a comparison of plasticized heat of melting values in PAN fibres.

4.2. Transformation of structure during carbon fibre manufacture

During oxidative stabilization and subsequent carbonization of PAN-based precursor fibres, the linear chain structure is transformed to a planar structure. Rings are formed due to the cyclization of nitrile groups of PAN during stabilization, followed by their aromatization and condensation during carbonization to give planar sections oriented along the fibre axis. The new structure is a consequence of chemical as well as morphological transformations.

4.2.1. Transformation during stabilization

Wide- and small-angle X-ray and electron diffraction have been employed to study the morphological changes during stabilization. The intensity of the main equatorial reflection at $2\theta = 17°$ from the (1 0 0) planes of PAN lattice shows an initial increase followed by a continuous decrease during stabilization [17, 158]. The spreads of the (1 0 0) reflection in the radial and azimuthal directions have been used to estimate the size and the orientation, respectively, of the laterally ordered phase in the precursor. Subsequent changes in them during stabilization of the precursor have been measured as a function of stabilization time or stabilization temperature. The method, however, is limited to the early part of stabilization due to complete disappearance of this reflection towards the end of stabilization. Rose [17] observed an initial increase followed by a continuous decrease in the orientation of the ordered phase as a function of heat-treatment temperature during stabilization in air. Thorne and Majoram [176] observed similar trends as a function of extent of reaction carried out in a nitrogen atmosphere, estimated by the amount of reacted nitrile groups from infrared spectroscopic measurements. They also studied the changes in the birefringence of precursor fibres during their heat treatment. A high birefringence of the new species formed as a result of chemical reactions would result in the high birefringence values of the annealed fibres even when the overall orientation remains unchanged. The data of Thorne and Marjoram, when replotted to give the birefringence of the species appearing in stabilization, indicate that the orientation of the new species appearing throughout the conversion is significant and that this orientation lies within a narrow range (Fig. 3).

Use of small-angle X-ray scattering (SAXS) has also been described in the literature for characterizing the morphological changes during stabilization. Such studies, although useful in identifying the superstructure which exists in the precursor fibres, reveal very little in terms of the morphology of the stabilized fibres. SAXS studies with wet-spun acrylic fibres show scattering from microvoids that is typical of wet-spun fibres [177, 178]. The characteristic long period reflecting a periodic density fluctuation which one normally observes in oriented synthetic fibres is, however, absent in these fibres. If the difference between the densities of the laterally ordered domains and the regions where such order is absent is very small [172, 173], SAXS would fail to differentiate between the presence and absence of any ordered sequence of these domains. Upon heat treatment of acrylic fibres in air or in an inert atmosphere, a meridional reflection appears which corresponds to a length of 8 to 16 nm of the scattering unit [158, 178–181]. The lateral dimensions of this scattering unit, calculated from the breadth of the reflection using the Scherrer equation, was found to be of the order of 6 nm [178, 179]. The intensity of this reflection goes through a maximum with time or temperature of heating.

According to Fillery and Goodhew [178], the spacing corresponding to the meridional streak varied with the precursor type, being 9.8 and 16.3 nm in the case of Courtelle and Dralon-T fibres, respectively. A size of 8 nm has been reported by Tyson [179] when unspecified commercial fibres were employed. Hinrichsen [180] also studied a number of commercial fibres and found apparent long periods ranging from 11 to 16 nm. When Dralon-N fibres drawn at 100° C were employed, the shape and size of the meridional reflections varied with the precursor draw-ratio, suggesting that the precursor morphology plays an important role in the development of long period. Warner *et al.* [158] studied the SAXS from two commercial fibres, coded fibre M containing 7% vinyl acetate and fibre C containing a small amount of an acid comonomer. The maximum intensity of meridional reflection was observed after 90 min in fibre M as opposed to 20 min in fibre C when heated at 220° C in air. The corresponding spacings in the two cases were 13.9 and

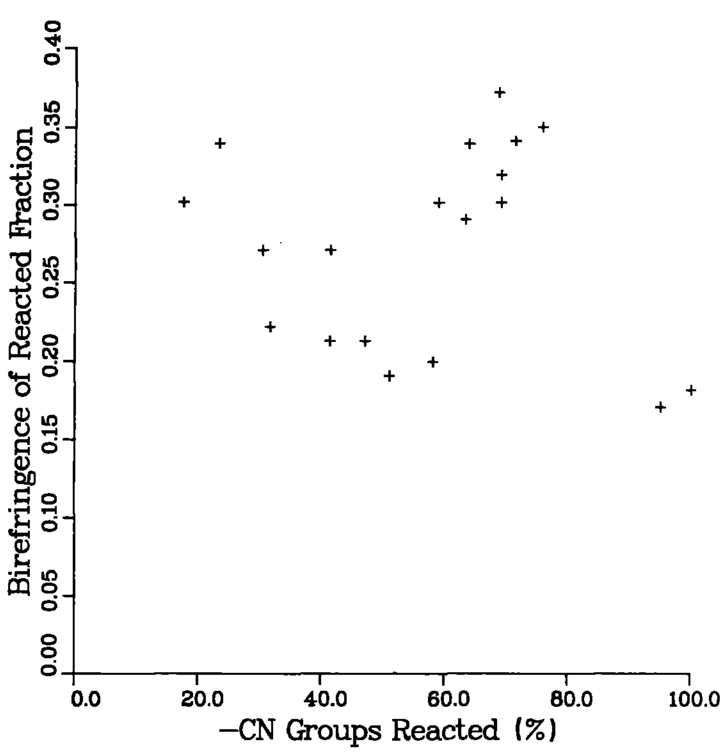

Figure 3 Replotted data of Thorne and Majoram [176] showing the birefringence of species appearing in stabilization.

8.8 nm, respectively. They explain the observed differences in intensity and spacing of the meridional reflections in the two commercial fibres in terms of both the differences in the stabilization mechanisms due to the different comonomers present in them and the possibly different starting morphologies of the two precursors.

The origin of the apparent long period observed in the above studies has not been shown precisely. Tyson suggests recrystallization and chain folding as the cause for the appearance of long period during pyrolysis. Fillery and Goodhew believe that the scattering intensity is controlled by the unreacted inner core and is influenced by the fibre diameter. Hinrichsen [180] proposes the intensification of the two-phase structure as a result of annealing close to the melting point and/or a change in the density of one of the phases due to selective reaction, either within the more ordered or in the less ordered regions, as the cause for the long period. As the chemical reactions proceed in the other phase, the density difference will diminish resulting in the disappearance of the long period in the later stages of stabilization. This explanation seems to be consistent with the appearance and disappearance of the long period.

4.2.2. Transformation during carbonization

During the carbonization stage, basal planes oriented along the fibre axis are formed, giving rise to the appearance of diffuse low intensity peaks at $2\theta = 26°$ and 44°. These reflections are indicative of relatively low lattice order and may be regarded as incipient (0 0 2) and (1 0 0) reflections of the graphite-like structure. The layer planes possess an interplanar distance of approximately 0.34 nm in carbon fibres (see Table I), slightly more than in pure graphite. This distance between the layer planes is indicated by $c_0/2$ based on the terminology used in X-ray studies of

TABLE I Wide-angle structural parameters for carbon fibres

C-fibre type	HTT* (°C)	Young's modulus (GPa)	L_c (nm)	$c_0/2$ (nm)	Z	$-q$	$L_{a\parallel}$ (nm)	$L_{a\perp}$ (nm)	Reference
GY-70	–	530	9.0	0.342	–	–	–	–	[218]
Type I	2500	390	5.3	0.350	20	0.78	9.8	8.0	[188]
Type II	1500	250	1.7	0.360	41	0.55	3.9	2.7	
Type III	1000	210	1.2	0.370	41	0.51	3.2	1.9	
Type I	2700	–	–	–	–	–	11.9	6.4	[199]
Type II	1250	–	–	–	–	–	3.5	3.4	
RR	2800	434	6.0	–	–	–	7.0	–	[189]
	2400	386	4.0	–	–	–	6.2	–	
	2400	338	3.4	–	–	–	5.4	–	
	1400	248	1.8	–	–	–	3.5	–	
	1000	214	1.0	–	–	–	2.0	–	
C	3000	483	11.2	0.3397	–	–	14.2	13.9	[170]
B	2750	434	9.3	0.3408	–	–	13.0	12.2	
A	2500	400	7.0	0.3414	–	–	8.8	8.1	

*Final heat-treatment temperature during their manufacture.

carbon and graphite (Fig. 4). The structure in carbon fibres lacks three-dimensional order and is termed "turbostratic graphite". The layer planes in a turbostratic structure are randomly rotated with respect to each other, as shown in Fig. 4b. The stack height of the layer planes, L_c, has been estimated from the radial spread of the (0 0 2) reflections by substituting the full width at half maximum (FWHM) intensity, B_{002}, in the Scherrer equation [178],

$$L_c = K\lambda/(B_{002} \cos \theta)$$

where λ is the wavelength of X-rays and θ is the Bragg angle. K, the Scherrer parameter, can be considered as a factor by which the apparent size must be multiplied to obtain the true size. For $(0\,0\,l)$ type reflections, K is generally given the value of 0.9 for FWHM or 1.0 for integral breadth. The (1 0 0) reflection is spread into a ring because of the turbostratic packing of graphitic layers. The layer plane length, L_a, parallel to the fibre axis is given by substituting the meridional width $B_{100}(\mathrm{m})$ in the Scherrer equation. Similarly, the equatorial width $B_{100}(\mathrm{e})$ is used to obtain the layer-plane dimension, $L_{a\perp}$, perpendicular to the fibre axis. K values for $(h\,k\,0)$ reflections vary with preferred orientation and have been evaluated by Johnson [183] and by Ruland and Tompa [184, 185]. The azimuthal spread of the (0 0 2) reflection is caused by the presence of misoriented crystallites. Intensity measurements in the azimuthal direction can be converted to a parameter, q, which varies from $+1$ for perfect orientation perpendicular to the fibre axis, through 0 for random orientation, to -1 for perfect orientation parallel to the fibre axis [186]. A simpler and more commonly used parameter for preferred orientation is Z, the FWHM in degrees, which is a measure of the average misalignment of the basal planes with respect to the fibre axis. The average tilt angle of the basal planes from the fibre axis is approximately $Z/2$.

Both L_c and L_a have been found to be low, of the order of 1 to 1.5 nm and 1.5 to 2.5 nm, respectively, up to a carbonization temperature of 800° C [34, 187]. A slight tendency towards increase in L_a from 1.9 to 2.5 nm during pyrolysis between 320 and 800° C has been reported by Watt *et al.* [34]. The dimensions of L_c and L_a, however, increase significantly upon graphitization. Table I lists various WAXD parameters for PAN-based carbon fibres obtained by different researchers. A general trend of increase in stack height and orientation of basal planes with increase in the heat-treatment temperature is quite evident [188, 189].

A relationship between the Young's modulus of carbon fibres, corrected for porosity using the assumption that the effect of pores on the modulus is essentially only an increase in the fibre cross-section,

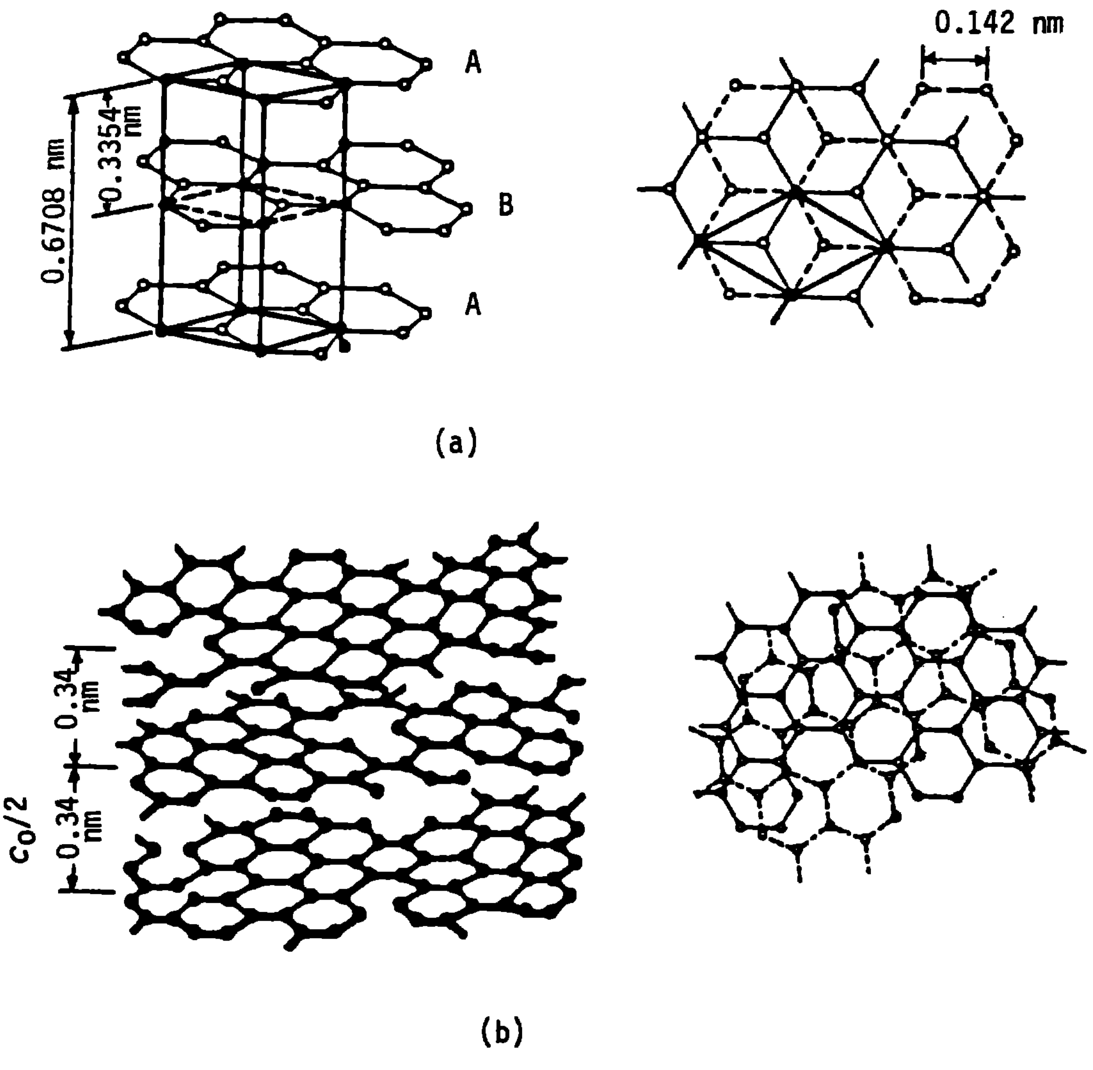

Figure 4 Arrangement of basal planes in carbon. (a) Graphitic carbon, (b) turbostratic carbon.

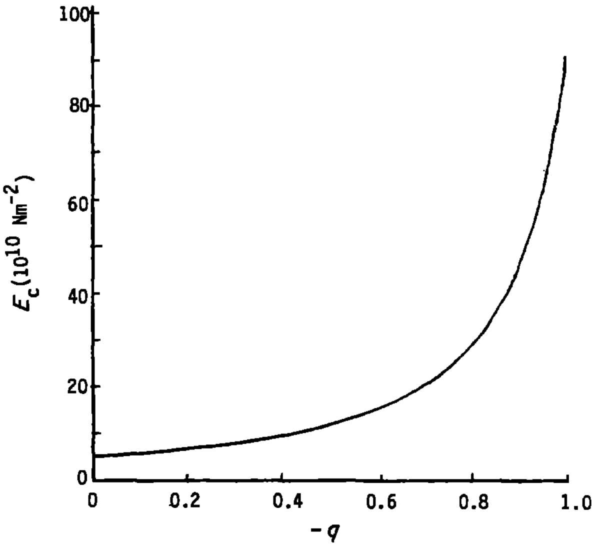

Figure 5 Plot of Young's modulus against orientation parameter of carbon fibres (Ruland [191]).

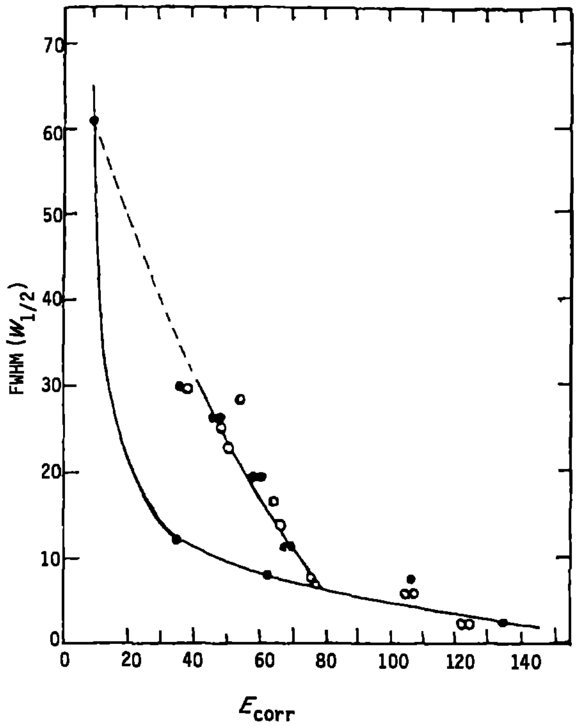

Figure 6 Plot of FWHM ($w_{1/2}$) against Young's modulus of carbon fibres. (Diefendorf and Tokarsky [192]). (●) Rayon base, (○) Courtelle PAN, (●●) Orlon PAN, (○○) experimental PAN.

and the orientation parameters has been observed by Fischer and Ruland [190, 191] (Fig. 5). This relationship, according to their observations, holds for carbon fibres of various precursors, heat treatments and preferred orientations. Diefendorf and Tokarsky [192], on the contrary, observed that only cellulose-based carbon fibres adhere to the Ruland-type relationship, while PAN-based fibres show a significant deviation (Fig. 6). This difference, they suggest, is caused by a gradient in preferred axial orientation present in PAN-based carbon fibres.

Skin-core heterogeneity in high modulus carbon fibres has been studied by Johnson's group [193–195] by measuring structural parameters in the interior and the surface from selected-area electron diffraction patterns after the application of peak resolution procedures. The crystallites in the skin (about 5% of the radius of the fibre) were found to be larger and more highly oriented than those in the core. Wicks and Coyle [196, 197] studied the size and the orientation of layer planes at various depths in single carbon fibres thinned to a "pencil point" taper using a flame-polishing technique. The results using X-ray and electron diffraction techniques suggest an inner region or core characterized by a relatively low axial alignment and large crystallite size and an outer sleeve or sheath of material of high preferred axial orientation and low average crystallite size. The larger crystallite size in the core compared to the sheath, however, is in total contradiction to the observations by Bennett and Johnson [193] where the crystallites in the core region were found smaller than in the sheath.

The presence of micropores in carbon fibres is indicated by an intense lobe-shaped scattering in the small-angle X-ray scattering (SAXS) photograph. These pores are shown to thin and needle-like, being longer in general than the crystallites which bound them [198–201]. From small-angle powder diagrams, three small-angle parameters have been calculated by Johnson and Tyson [198, 200] using the methods of Debye and Porod [202–205]. Porod has defined a "distance of heterogeneity", l_p, in terms of the integral width of the correlation function $C(r)$ (which is related to the probability that a line of length r will have both ends situated in pores) as

$$l_p = 2\int_0^\infty C(r)\,\mathrm{d}r \quad \text{where } C(r) = \exp(-r/a)$$

a is a correlation length which can be determined from the slope to intercept ratio of the $I^{1/2}$ against θ^2 straight-line relationship (Fig. 7). The average chord lengths of the pore and the carbon region, l_p and l_c, respectively, and the surface area per unit mass inside the fibres, S_v, can then be calculated by using the relationships

$$l_p = 2a, \quad l_c = a/(1-D)$$

$$\text{and} \quad S_v = 4D(1-D)/a$$

where D is the fraction of fibre occupied by carbon, usually approximated by the ratio of the fibre density to the bulk graphite density. More rigourous methods which make use of the small-angle fibre diagrams have been described by Perret and Ruland [199, 201]. Table II lists the values of the above small-angle structural parameters in PAN-based carbon fibres reported by various authors. No comparisons between different data are possible due to lack of details about the precursors and the conditions for their conversion to carbon fibres. In general, the results give an idea about the relative sizes of the pores and the crystallites, which have also been confirmed by electron microscopic measurements [134, 188, 190, 198, 206–208]. An increasing trend in l_p and l_c parameters and a decrease in pore surface area with increase in treatment temperature is quite evident from Johnson and Tyson's results [188, 189, 200]. Ruland [199, 209] has attributed the increase in l_p and l_c at high temperatures

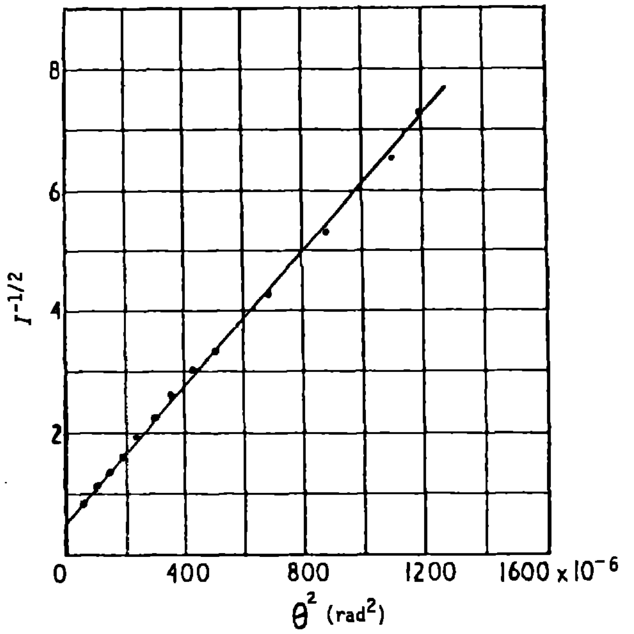

Figure 7 Plot of $I^{-0.5}$ against θ^2 for low-angle powder-type diffraction from graphitized fibres Type A [198].

to the elimination of smaller pores, with a simultaneous increase in the crystal size through "elastic unwrinkling". The fraction of pores is about 10% of the total volume of fibres, which is of the same order as the value (15%) of internal porosity closed to helium gas reported by Spencer *et al.* [210].

4.3. Structure of carbon fibres

The structure and properties of carbon fibres depend on several factors, the most important of which are the heat-treatment temperature (HTT) and the type of precursor used. Among polyacrylonitrile (PAN)-based carbon fibres, two types, i.e. high modulus or type I (2500 to 3000° C) and high strength or type II (1200 to 1600° C), have been widely employed for detailed structural studies. The development of structure in carbon fibres, which also decides their properties, depends on the process conditions employed during their manufacture. A knowledge of fibre structure in three dimensions, from the scale of the fibre diameter to at least the ultra-structural level, is therefore essential if the process is to be optimized for desired fibre properties. The moduli of individual fibres will depend on the details of the preferred axial orientation in each fibre structure, while the strength will be a function not only of preferred orientation but also of the flaws and the textures and the gradients in structure present. The techniques employed for structure determination in carbon fibres include electron spin resonance [207, 208], neutron [213], electron and X-ray diffraction and optical and electron microscopic examinations.

Optical microscopy of thin transverse sections of carbon fibres from fully stabilized Courtelle and Orlon fibres displayed extinction crosses when viewed under polarized light which, according to LeMaistre and Diefendorf [214], suggest an onion-skin type cross-section with the basal plane showing a preferred orientation parallel to the fibre surface. Commercially produced carbon fibre, on the other hand, displayed a radial texture in the core while a circumferential orientation of basal planes was present in the sheath. Wicks and Coyle [197] have reported at least four types of layer plane arrangements in various filaments of a commercially produced tow of high modulus PAN-based carbon fibres. Knibbs [215], however, has claimed that by varying the process conditions, the type of texture can be altered, varying from a circumferentially arranged sheath with an isotropic or radially oriented core to a circumferential orientation throughout the cross-section. The skin–core heterogeneity in high modulus carbon fibres has been confirmed by others with scanning electron microscopy (SEM) of fractured [192, 193, 197, 216, 217] and oxygen plasma etched [217, 220] specimens. Johnson [221], on the contrary, discounts the presence of radial heterogeneity and has proposed a random arrangement of crystallites. According to his experiments, similar amounts of erosions were observed in the sheath and core upon etching with argon ions for short erosion times (less than 60 min) and they appeared uniform in electron microscopical observations. He suggests that the Maltese cross pattern observed in the polished cross-sections of carbon fibres is caused not by structural anisotropy but by strain birefringence. The radial stresses in the fibre cross-section which lead to strain birefringence are probably caused by the differential shrinkage, during

TABLE II Structural parameters for carbon fibres from SAXS studies

C-fibre type	HTT* (° C)	Young's modulus (GPa)	l_p (nm)	S_v (m^{2}cm^{-3})	l_c (nm)	Reference
GY-70	–	530	1.6	490	7.3	[218]
Type I	2500	390	2.5	–	–	[188]
Type II	1500	250	1.4	–	–	
Type III	1000	210	0.9	–	–	
Type I	2700	–	1.5	226	12.4	[199]
Type II	1250	–	0.7	454	6.4	
RR	2800	434	2.8	340	10.0	[189, 200]
	2400	386	2.9	363	8.6	
	2000	338	2.5	485	6.7	
	1400	248	1.2	1100	3.4	
	1000	214	0.9	1450	2.6	

*Final heat-treatment temperature during their manufacture.

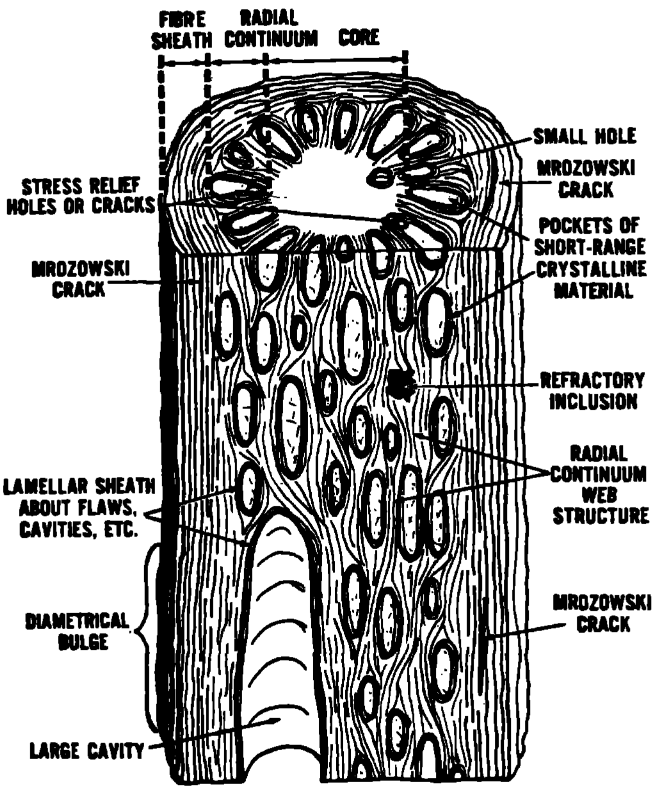

Figure 8 Structural model of carbon fibres by Barnet and Norr [220].

carbonization and subsequent cool down, between the oxygen-rich surface and the partially oxidized core. A three-dimensional structural model for high modulus PAN-based carbon fibres was proposed by Barnet and Norr [219, 220] based on electron microscopical observations of oxygen plasma-etched fibres. The artefacts produced by etching were interpreted as originating from a highly crystalline sheath surrounding a radial structure of crystalline webs separated by large voids (Fig. 8).

Several other structural models of carbon fibres have been proposed by various researchers [198, 199, 214, 222–225]. These models are based on X-ray and electron microscopical examinations of carbon fibres. A schematic illutration of the model proposed by Johnson and Tyson [198, 200], based on the wide- and low-angle X-ray scattering of high modulus carbon fibres is shown in Fig. 9. The idealized tetragonal-shaped crystals, approximately 7 nm in size, enclose sharp-edged voids, about 1 nm wide. Extinction bands orthogonal to the crystal direction were observed in phase contrast microscopy which suggest the presence of subgrain boundaries between the crystals with both tilt and twist components. Perret and Ruland [199], however, disagree with this model and propose, based on their X-ray and electron microscopical observations, a ribbon-type structure for PAN-based carbon fibres. The basic unit of Ruland's model is a ribbon of sp^2 type carbon with an average width of 5 to 7 nm. The ribbons are slowly undulating and contain straight parts with lengths in the 6 to 13 nm range depending on the preferred orientation. An extensive parallel stacking of these ribbons, which has also been observed by others [134, 198, 206, 207, 218], is suggested. These ribbons pass smoothly from one domain of stacking to the other, as shown in Fig. 10. The space between the contours of these parallel stacks gives rise to needle-shaped pores or voids which are considerably longer than the average straight parts of the ribbons. Similar models have been suggested by Hugo *et al.* [213] and by Diefendorf and Tokarsky [192]. The structural units of the model proposed by the latter authors are microfibrils which are made of 10 to 30 basal planes in the form of ribbons (Fig. 11). For low

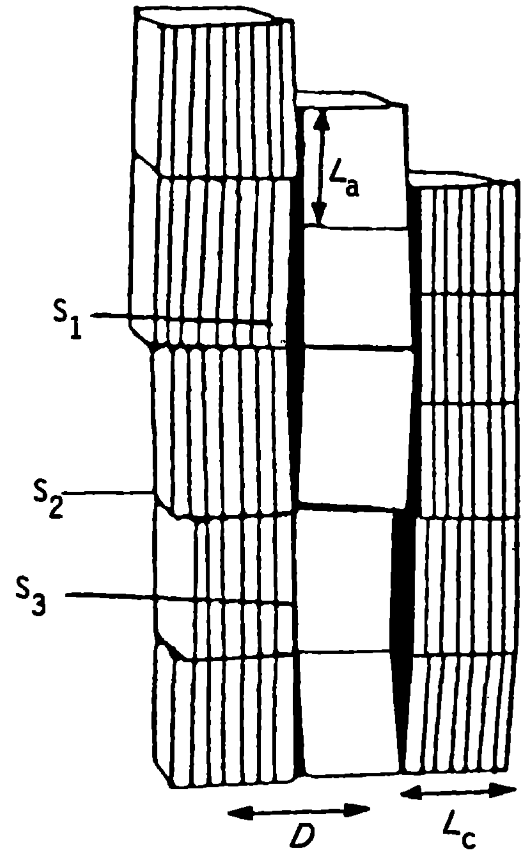

Figure 9 Model of carbon fibres; tetragonal crystals and sharp-edged voids [198].

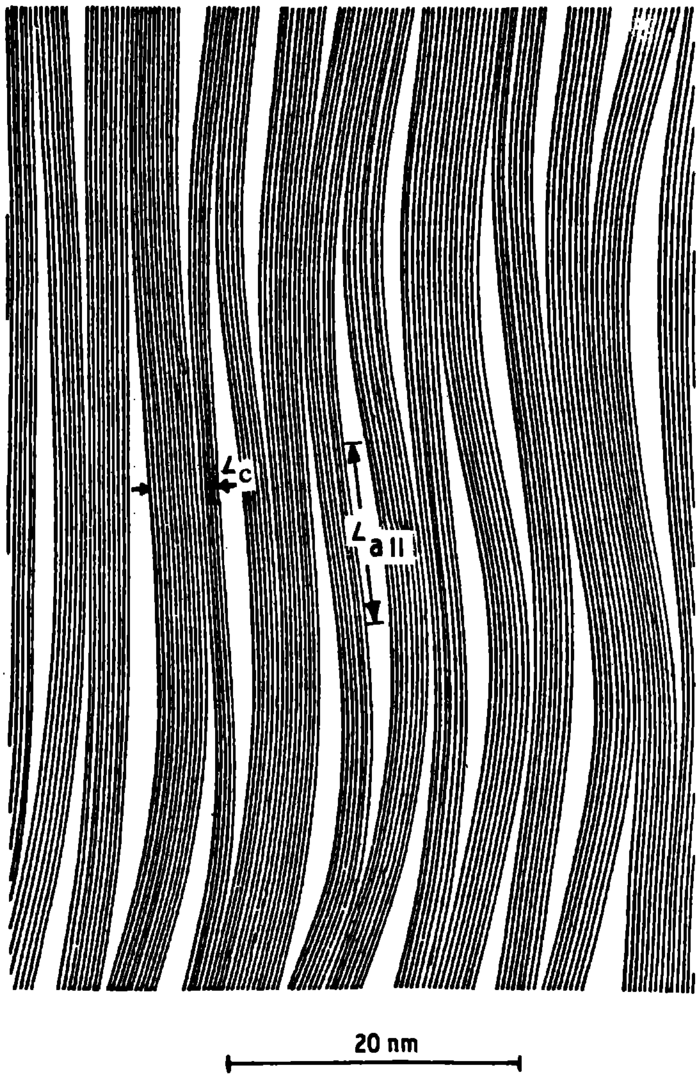

Figure 10 Ribbon model of carbon fibres suggested by Perret and Ruland [199].

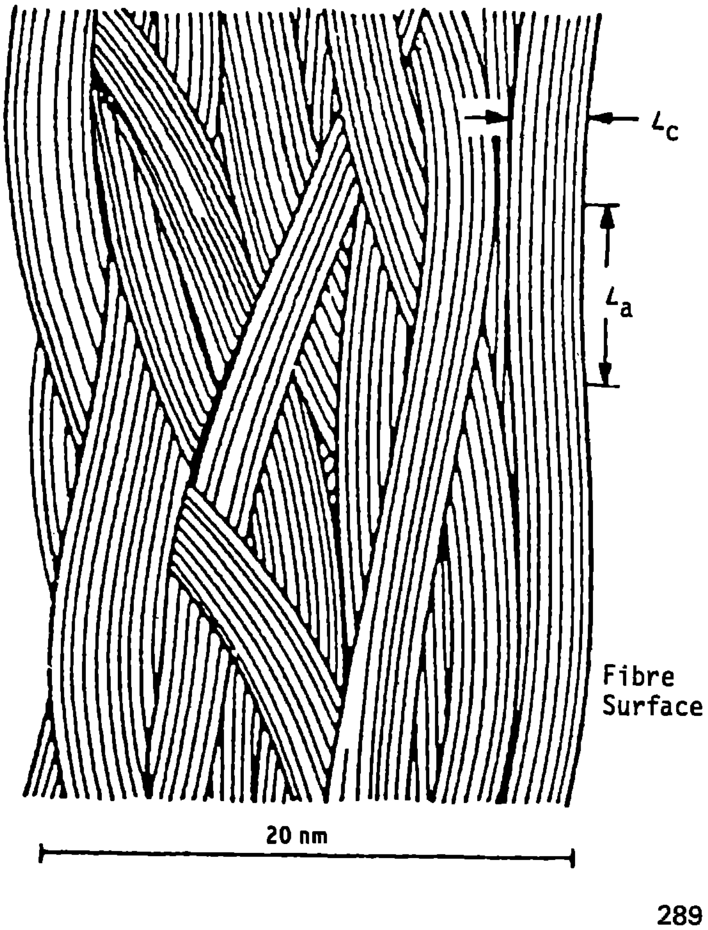

Figure 11 Structural model of carbon fibres suggested by Diefendorf and Tokarsky [192] showing microfibrils.

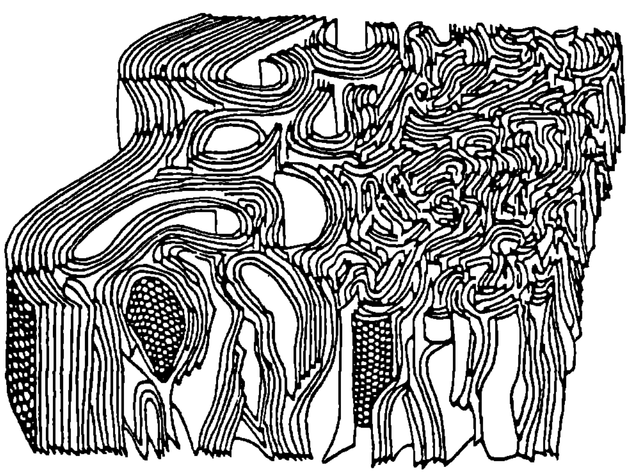

Figure 12 Schematic illustration of model derived by Bennett and Johnson from electron microscopic observations [194].

modulus (40×10^6 psi, $\sim 2.76 \times 10^5$ N mm^{-2}) fibres, the ribbons are typically 13 layer planes thick and 4 nm wide, whereas the corresponding dimensions increase to 30 layers and 9 nm for high modulus (100×10^6 psi, $\sim 6.89 \times 10^5$ N mm^{-2}) fibres. The microfibrils undulate, the amplitude of undulation being greater than the wavelength in high strength fibres, becoming smaller in high modulus fibres due to dewrinkling of the ribbons [224]. An increase in the orientation of (0 0 2) planes with increase in the fibre treatment temperature [186, 188, 208] supports this hypothesis. Based on their bright- and dark-field transmission electron microscopy (TEM) of high modulus fibres, Diefendorf and Tokarsky [192] and Oberlin *et al.* [225] proposed that wrinkled sheets rather than ribbons describe better the structure in these fibres. A schematic model, as shown in Fig. 12, was drawn by Bennett and Johnson [194] after combining the observations from high-resolution electron microscopy which included dark- and bright-field image analysis and specimen tilting procedures. The layer planes in crystallites, oriented along the fibre axis, are shown to interlink in a highly complex manner, giving a range of crystallite sizes enclosing an intricate void system.

In addition to the microfibrillar structure discussed in the preceding paragraphs, morphological features with dimensions much larger than those of the microfibrils have been observed in microtomed sections of carbon fibres of various origins and degrees of graphitization [134, 206, 207, 226]. They are usually referred to as secondary fibrils and their dimensions are estimated to be in the range 20 to 100 nm. Mencik *et al.* [227], however, based on their low-resolution TEM studies, suggest that secondary features larger than the graphite fibrils [1.5 to 15 nm) are artefacts created by the interaction of the knife with the fibres during microtoming.

The observations of carbon fibre structure by various researchers are contradictory at times. In most cases, the type of precursor fibres, their structure and conditions for converting them to carbon fibres are not disclosed. It is known that these parameters have substantial influence on the development of structure in carbon fibres. The concept of basal planes forming ribbons or sheets, arranged parallel to the fibre axis direction in some fashion, has been well substantiated from X-ray and electron microscopic studies by several workers. A sheath–core structure having different arrangements of these basal planes in the skin and the inside seems possible with certain precursors and processing conditions, while some other precursor and conditions could as well result in an isotropic cross-section of the carbon fibres. It would be erroneous to presume that the morphologies of all the carbon fibres produced from different precursors and under different conditions would correspond to any one of the proposed morphological models.

5. Tensile properties of carbon fibres

5.1. Methods of testing

For comparing the tensile strengths of various carbon fibres, it is important to understand the test methods involved and the test specimen used. The tensile testing of single filaments is laborious because of the fragile nature of the fine filaments (typically 6 to 10 μm diameter). The method has, however, been used extensively in testing experimental fibres in research and development. There is a standard ASTM specification (ASTM-3379-75) for the preparation, mounting and testing of high modulus single filament materials of over 20 GPa (3×10^6 psi) Young's modulus. In testing yarns and tows comprising many hundreds or thousands of filaments, a portion of the tow is selected which is passed through a resin bath, dried and cured. The cured specimens in the form of rods are then tested using a tensile tester with rubber-faced clamps for tight grasping of these composite rods without crushing. Alternatively, a large diameter collar of liquid resin, fitting within a smaller receptacle on the testing machine, is cast on the exposed fibre ends for a good grip while testing [228–229]. Dry strand testing of fibres was pursued by McMahon [230], who compared the test data of the impregnated strands of carbon fibres with dry strand techniques. Good correlation of test results was reported by him for the tensile strengths in the two cases. In continuous manufacture of carbon fibres it is useful to be able to measure mechanical properties continuously since this will give an immediate indication of any change in the process. Methods for on-line measurement of Young's modulus of carbon fibres include measurement of the electrical resistivity [231] and determination of transit time for short ultrasonic pulses along the fibre bundle [232], which are then converted to elastic modulus through the use of predetermined correlations.

5.2. Development through stabilization and carbonization

The tensile properties of the precursor fibres change continuously during stabilization and carbonization. The stress–strain plot of a precursor fibre shows an initial elastic portion with a definite yield point followed by a regime of plastic deformation with increasing resistance to deformation until fracture occurs. The initial elastic region has been explained by Rosenbaum [233] to be due to reversible straightening of twisted molecules against intra-molecular repulsion of adjacent dipoles. The chains start to move relative to each other at the yield point because the cohesive energy between the chains is overcome. According to Watt [55], the flow and straightening of non-aligned chains causes a more equal distribution of load between the chains so that the cohesive energy of more dipoles have to be overcome which accounts for the increasing resistance to flow until the fibre finally breaks.

Unidentified precursor fibres, when oxidized at 220° C for 5 h, showed the same initial elastic portion as the original fibre followed by a steep plastic deformation region, which has been attributed by Watt [55] to a decrease in the cohesive energy between the chains. The decrease in cohesive energy results from the conversion of highly polar nitrile groups to the less polar $>C=N-$ groups upon oxidation. Bahl and Manocha [39, 234] observed a continuous decrease in the tensile strength of acrylic fibres upon heating in oxygen which they have attributed to the chemical changes as suggested by Watt. The primary or initial modulus of the precursor fibre decreased suddenly after 9 h heating at 205° C and continued to decrease thereafter. A continuous decrease in the tensile strength, tensile modulus and extension at break with increase in temperature of Courtelle fibres above 200° C in argon has been reported by Turner and Johnson [30]. Similar experiments by Ferguson and Mahapatro [235, 236] on some experimental fibres showed quite different results as a function of pyrolysis time. The initial modulus as well as tenacity went through a maximum whereas extension at break fell rapidly to low values upon pyrolysis at 220° C under a slight tension. A similar trend was observed by Russian workers [237] as a function of the temperature of heating between 150 and 200° C in air. These changes have been associated with chemical changes by Ferguson and Mahapatro. In support, they have shown that the ratio of the absorbances at 6.29 μm due to $>C=C<$ and at 3.12 μm due to end groups such as $-COOH$ and $-CONH$ in infrared spectroscopy, which is a measure of the ratio of cyclization to degradation, also goes through a maximum with pyrolysis time. The same fibres, when drawn 700% at 100° C and pyrolysed, showed different trends [236]. The changes in initial modulus were dependent upon the form of constraints imposed during pyrolysis, an initial increase followed by a decrease under constant load conditions (0.35 g tension was applied on filaments of unspecified denier) and a sharp decrease under constant length pyrolysis. Breaking strength showed a continuous decrease while elongation at break first increased and then decreased under both conditions. The different behaviour of the drawn fibres has been attributed by Ferguson and Mahapatro to the occurrence of different degrees of molecular relaxation processes along with the chemical changes during pyrolysis. The effect of molecular weight of the original polymer on the changes in the tensile properties of fibres with pyrolysis at constant load has also been shown by them. Takaku *et al.* [142, 143] measured tensile modulus during air heating at various temperatures, by extending the specimen to a small elongation, measuring the stress and immediately releasing it. This measurement, when carried out on a specimen which was heated at the rate of $1°\,C\,min^{-1}$ showed a decrease in tensile modulus up to a temperature of approximately 200° C after which it increased. Isothermal heating in excess of 200° C showed an increase in modulus with increasing heat-treatment time, with a tendency to level off at longer times. The curves shifted towards shorter times with increasing temperature. Rate constants at various temperatures were calculated by Takaku *et al.* from the above curves which gave an apparent activation energy of $98.3\,kJ\,mol^{-1}$.

With the exception of Takuku *et al.*'s experiment where the initial modulus was measured during heating of the precursor [142, 143], the tensile strength, Young's modulus and elongation at break of the stabilized fibres have been found to be less than those of the starting precursor fibres. Except for the elongation at break, these properties start improving when the stabilized fibres are subjected to high temperatures in an inert environment during carbonization. According to Watt [55] and Watt and Green [70], strength and modulus were found to increase on pyrolysis around 300° C and continued to increase monotonically up to 1000° C. Heat treatment at temperatures higher than about 1500° C usually results in a decrease in tensile strength [33, 119–123] whereas the Young's modulus continues to increase up to 3000° C. This decrease in tensile strength has been attributed by Reynolds and Moreton [238] to the surface flaws originated from dust particles on the fibre surface by their reaction with the fibre surface itself at these high temperatures. When precursor fibres spun in clean room conditions were used, the tensile strength of carbon fibres was found to increase continuously up to a heat-treatment temperature of 2500° C [239].

5.3. Dependence on precursor properties

The quality of the ultimate carbon fibre depends on the precursor properties and on the stabilization and carbonization conditions. For a given chemical composition of the precursor, the properties of carbon fibres are decided by the properties of the precursor, provided the same stabilization and carbonization conditions are employed. The spinning and the drawing history of the precursor fibres plays an important role. Moreton [240], from his studies of carbon fibres made from copolymer fibres, which were wet spun from an inorganic system and drawn 5 to 13 times in steam, concluded that the tensile strength and modulus of carbon fibres are directly related to the stretch ratio of the precursor (Table III). When glycerol at 130 and 150° C was substituted for steam as the drawing medium, a significant improvement in the tensile properties of the precursor fibres was observed. These fibres possessed larger crystals and on conversion to carbon fibres showed better tensile strength and modulus than those from steam-drawn fibres [241]. Increasing the glycerol bath temperature to 160° C resulted in a deterioration in the properties of the precursor as well as the carbon fibres made from them. Similarly the properties of carbon fibres made from very highly drawn (22 × in glycerol) fibres were

TABLE III Results of Moreton's studies – 6% methacrylate copolymer

Draw ratio	Drawing temperature (° C)/medium	Precursor fibres		Fibres carbonized at 1000° C		Fibres carbonized at 2500° C		Reference
		Tensile strength (GPa)	Young's modulus (GPa)	Tensile strength (GPa)	Young's modulus (GPa)	Tensile strength (GPa)	Young's modulus (GPa)	
5	100/steam	0.18	3.78	0.84	101	0.68	213	[240]
6	100/steam	0.20	4.20	0.78	105	0.55	248	
8	100/steam	0.27	5.51	0.92	130	0.83	282	
9	100/steam	0.30	5.64	0.94	124	0.83	283	
13	100/steam	0.59	9.64	1.14	154	1.22	345	
14	100/steam	0.61	15.20	1.50	227	1.32	427	[241]
14	130/glycerol	0.63	16.50	1.51	241	1.78	461	
14	150/glycerol	0.85	18.60	2.19	255	1.98	448	
14	160/glycerol	0.83	17.90	1.71	255	1.52	448	
22	150/glycerol	1.14	19.30	1.86	241	1.41	448	
14/clean*	100/steam	0.55	10.40	2.19	186	2.75	380	[239]
14/control	100/steam	0.65	13.00	1.95	172	1.51	366	

*Specified clean-room conditions (less than 100 particles/ft^3 at 0.5 μm and above, none > 5 μm).

inferior to that from 14 × drawn fibres even though the former possessed better tensile strength and modulus than the latter in the precursor form. Moreton has explained it in terms of overstretching of precursor which leads to the generation of defects upon carbonization. This discrepancy could also be explained in terms of the overstabilization of the 22 × drawn fibres. Since the same stabilization conditions were used by them for various precursor fibres which had different deniers, it is quite possible that the 22 × drawn fibre of much lower filament denier was overstabilized, thus giving inferior properties on carbonization when compared with the 14 × drawn fibre.

Ishikawa *et al.* [242, 243] stretched precursor fibres up to 280% in steam before converting them to carbon fibres and found that the strength and modulus of carbon fibres prepared by carbonization at 2500 to 3000° C increase with increase in the draw ratio of the precursor. Similar results have also been reported recently in 1100 to 1350° C treated carbon fibres by Fitzer and Muller [244], Radhakrishnan *et al.* [245] and Nagabhushanam *et al.* [246] from precursor fibres drawn to different draw ratios. Fitzer and Muller emphasize the fact that each stretch ratio needs an individual optimization of the stabilization time. This aspect has been ignored by most previous workers trying to correlate precursor properties with carbon fibre properties. Other attempts to study the effect of precursor composition [104, 247, 248] and the type of spinning (wet compared to dry) [249] on carbon fibre properties have been made by various workers. A direct relationship between the Young's moduli of various PAN-based commercial precursors and the carbon fibres produced from them were observed by Chari *et al.* [250]. The ratio of carbon fibre to precursor fibre modulus was found to be approximately 20. Based on the WAXD patterns of three commercial precursor fibres, Beslon, Courtelle and Toray, they also recommend that the longitudinal order, as seen in the Beslon fibres should be avoided since it hinders the process of molecular chain orientation during the preoxidation stage, thus giving carbon fibres with inferior properties [251]. Their conclusion, however, is based only on the fact that slightly lower modulus is obtained in carbon fibres from Beslon fibres than that from Courtelle fibres. They have unjustifiably ignored the chemical composition and the spinning history of these precursors, which could significantly influence the properties of carbon fibres.

5.4. Dependence on process conditions

In addition to the dependence on precursor properties, the stabilization and carbonization conditions such as the time, temperature and rate of heating and the dimensional constraints imposed during these processes have a significant influence on the final carbon fibre properties. Influence of the air flow rate during stabilization of commercial acrylic fibres from Courtaulds on the Young's modulus of carbon fibres has been reported recently by Nagabhushanam *et al.* [246]. A decrease in the Young's modulus of the carbon fibres, prepared by carbonization at 1100° C, was observed when the air flow was increased from zero to 35 $1\,\text{min}^{-1}$ during stabilization. This decrease was negligible when the above precursor was drawn by 15% at 190° C before converting it to carbon fibre. The effect of stabilization temperature on the carbon fibre properties was studied by Bahl and Manocha [39] where they employed stabilization temperatures of 205 and 215° C in oxygen, while a constant load of 0.1 g/denier was applied which caused extensions of 12 and 16%, respectively, in the two cases. The 20% higher strength of carbon fibres reported by them when a higher stabilization temperature was employed could have resulted from increased orientation due to tensile deformation during stabilization.

Time of oxidative stabilization should be optimized for a given temperature and precursor, since under- or over-stabilization could result in loss of properties of the final carbon fibres [33, 234]. The observations by Bahl and Manocha [39] and by Watt and Johnson [33], where the tensile strength of carbon fibres went through a maximum with stabilization time, show this very clearly. Various chemical and physical methods have been employed to ascertain optimum stabilization. In addition to the measurements of unreacted nitrile groups [53, 252], density [30, 114, 176, 253], oxygen pick-up [33, 91, 92, 96, 97, 99] moisture pick-up [32, 85] and per cent shrinkage [93, 140, 254] have also been employed frequently as quality control measures. Layden [99] has defined an optimum time for stabilization at a given temperature as the time when the oxygen pick-up of the fibre approaches 10%. Based on experimental data, he has suggested empirical relationships to calculate the time for optimum stabilization for homopolymer fibres in air. Bahl and Manocha [38] have supplemented these equations by additional equations to include the copolymer fibres and oxygen environment. Their optimization is, however, based on a free shrinkage of 24% in precursor fibre.

The load and elongation during stabilization of precursor fibres have been shown to affect the final carbon fibre properties. A continuous increase in tensile strength and modulus of carbon fibres was observed by Ishikawa *et al.* [242] when increasing tensions up to 0.16 g/denier were applied during stabilization. Watt and Johnson [33, 134] also witnessed an improvement in the properties of carbon fibres with increase in load during stabilization of Courtelle fibres. Extensions of up to 40% were observed during this stage upon application of up to 0.15 g/denier tension. The changes in properties were more dramatic for carbon fibres treated at 2500° C than for the fibres produced at 1000° C. Since the extent of stretching is more when a higher load is applied [33, 134, 242] or when a higher temperature is used [39] during stabilization, the stabilized fibre will posses a higher orientation which will ultimately lead to carbon fibres with higher orientation and thus superior tensile properties. Contrary to the observations by other workers, Bahl and Manocha [139], from their experiments with Beslon fibres, showed that both the tensile strength and modulus of carbon fibres go through a maximum when plotted against load applied during preoxidation. The best properties were obtained at a tension of approximately 0.1 g/denier corresponding to about 7% shrinkage during oxidation. The decrease in properties at loads higher than an optimum load results, according to them, from bond rupture during the preoxidation stage. A further improvement in carbon fibre properties was obtained by applying a low (0.015 g/denier) tension during a programmed heating of the precursor fibres to 240° C followed by 0.1 g/denier tension during a 100 min soak-up period at this temperature. The properties of carbon fibres are also influenced by the application of load or stretching during carbonization. When an unspecified load corresponding to a shrinkage of 3 to 8% was applied during carbonization of a fully stabilized precursor fibre at 1000° C, a small increase of about 10% in strength and modulus of carbon fibres was observed by Manocha *et al.* [37]. Experiments by Ezekiel [126], where different tensions were applied during carbonization at 2500 to 2900° C, showed only minor changes in tensile properties of carbon fibres, whereas stretching of the fibres during carbonization resulted in significant improvement in their properties. W. Johnson [129] observed more than a 30% increase, from 60 to about 90 $\times 10^6$ psi, in the (~ 4.14 to $6.2 \times 10^5\,\mathrm{N\,mm^{-2}}$) Young's modulus of carbon fibres when stretched up to 28.6% during carbonization at 2500 to 2800° C. Similar results have also been reported by J. W. Johnson's group [128] where they observed a 20 to 30% increase in the tensile strength and modulus by stretching in the temperature range 2000 to 3000° C. The strength of the stretched carbon fibres showed a linear dependence on modulus while the unstretched fibres suggested no such relationship.

5.5. Flaw or defect dependency

Studies show that the tensile fracture in carbon fibres mainly originates at points of internal and surface irregularities or flaws. The tensile strength of PAN-based carbon fibres increases with decreasing gauge length due to the reduction of available flaws in the gauge length. Diefendorf [255] extrapolated such data and concluded that zero flaw carbon fibres would display tensile strengths in the range of 1.5×10^6 psi ($\sim 1.03 \times 10^4\,\mathrm{N\,mm^{-2}}$). Values of 10^6 psi ($\sim 6.89 \times 10^3\,\mathrm{N\,mm^{-2}}$) have also been predicted by Jones and Johnson [256]. This is still only about half the tensile strength obtained by Bacon [1, 2] in the case of carbon whiskers, which possess a high degree of crystalline perfection with no grain boundaries and very low dislocation density, void content and surface imperfections. The theoretically estimated tensile strength of these whiskers, using the modulus of elasticity obtained from vibrational measurements is 15×10^6 psi ($\sim 1.03 \times 10^5\,\mathrm{N\,mm^{-2}}$), approximately one-tenth of their modulus [257].

A number of studies were made in the early seventies of flaws or defects, their nature and their influence on the fracture behaviour of carbon fibres. The technology has advanced since then and the commercial carbon fibres currently in the market are more uniform and possess superior tensile properties (Table IV). Earlier work on the nature of defects or flaws in carbon fibres may not, therefore, relate fully to the carbon fibres produced today. A review by Reynolds [258] on the physical properties of carbon fibres describes the earlier research (up to 1973) on the dependence of tensile properties on surface and internal flaws.

Fracture mechanisms based on the shear stresses in the misoriented crystallites have been suggested by Stewart and Feughelman [259]. When the fibre is loaded to typical tensile loads, there is a high concentration of shear strain energy in the regions of enhanced misorientation of crystallites, which is believed to initiate cracks. Increased crystallization is also produced around the flaws making the initial crack propagation easier. In a recent paper by Bennett and Johnson [260], the emphasis is placed on the failure due to misoriented crystallites in the fibre rather than the flaw itself. Internal flaws which did not initiate failure were seen to have walls containing crystallites arranged mostly parallel to the fibre axis but the flaws which did initiate failure showed evidence of large misoriented crystallites in the walls of

TABLE IV Tensile properties of carbon fibres

Fibre type/ manufacturer	Year	Tensile strength (10^3 psi)*	Young's modulus (10^6 psi)	Comments	Reference
Data obtained from early publications					
Acrilan-based	1969	180	20	–	[262]
R.A.E. process	1969	309	24.9	HS/1500	[266]
		266	53.4	HM/2500	
Le Carbone Lorraine	1971	312	26.7	HS	[280]
		232	55.7	HM	
Watt, Philips and Johnson	1971	250	50	HM	[277]
Courtauld	1974	363	37.7	HTS/1500	[264]
		160	59.5	HMS/3000	
Recent data from various manufacturers					
Magnamite by Hercules Corp.	1984	635	40.4	Type IM6	
		600	35.3	AS6	
		320	50.0	HMS	
		400	55.0	HMU	
Celion by Celanese Corp.	1984	630	34.4	Type ST	
		515	34.0	C-6	
		270	75.0	GY-70	
Thornel by Union Carbide	1984	660	36.0	Type T-700	
		530	35.0	T-500	
		350	57.0	T-50	
		325	120.0	P-120†	
		325	105.0	P-100†	

*10^3 psi ≡ 6.89 N mm^{-2}.
†Pitch-based carbon fibres.

the flaws. They conclude that the presence of misoriented crystallites in the walls of the flaws rather than the flaw itself determines whether or not tensile failure will occur. In the absence of gross flaws, they have predicted breaking strains of 1 to 1.3% in high modulus and greater than 2% in high-strength PAN-based carbon fibres. Similar predictions have also been made by Jones and Johnson [256].

5.6. Nature and origin of flaws

Tensile test data on carbon fibres show variations in the Young's modulus and breaking strength values but the typical coefficient of variation for breaking strength is higher, about 25%, when compared with the variation in modulus which is only about 10% [261]. This large scatter in the breaking strength of carbon fibres has been associated with the surface and internal irregularities or flaws. In carbon fibres from Courtelle and Acrilan precursors, both surface and internal flaws were found responsible for premature brittle failure [262]. The majority of internal flaws were identified as elongated voids or cavities, 1 to 4 μm in width. The flaws were found distributed extremely unevenly in the fibre sample, with an average flaw concentration of approximately 8 per cm in Acrilan-based carbon fibres. A cathodic etching technique which employed argon ion bombardment was used by Johnson [119] to remove some of the fibre surface, thus producing a longitudinal section exposing the fibre interior. The voids responsible for failure were diconic in shape with the long axes parallel to the fibre length. These internal voids, it is believed, are produced by impurities in the precursor fibre, since PAN fibres spun with deliberately included particulate matter [263] also showed the diconic-shaped structures. According to Sharp *et al.* [264], the diconic-shaped flaws produce local misorientation due to the tendency of the basal planes to follow the contours of the flaws. These regions of enhanced misorientation are believed to be sources of weakness in the fibre.

The origin of surface flaws in carbon fibres has also been traced to the precursor fibre formation process by Murphy and Jones [265]. As the viscous polymer solution emerges from the spinneret during precursor spinning, they believe that some filaments stick together and also that droplets of polymer solution are deposited on the surface of the individual filaments. When the precursor tow is subsequently heat treated, both these can lead to defects on the surface. Scanning electron microscopy (SEM) of some commercial carbon fibres demonstrated the presence of surface deposits and joined fibres. Oxidation of these fibres at 680° C in air for 45 min changed the surface deposits to pits due to more rapid oxidation of these sites compared to the surface. Some of the fibres were found to have circumferential defects with shapes very similar to the shapes one would expect if the joined fibres were separated. It is difficult, however, to generalize from these isolated observations regarding universal sources of defects in carbon fibres. It was proposed by Johnson and Thorne that the surface flaws can be modified by argon-ion etching [119] or air oxidation [262] to improve the tensile strength of carbon fibres.

TABLE V Gauge length and tensile strength of carbon fibres

Source	Gauge length (cm)	No. of tests	Tensile strength (10^3 psi)*	S.D. (%)	Comments	Reference
Manufactured by R.A.E. (1968)	10.0	50	266	21.0	HM/2500	[266]
	5.0	50	300	28.0		
	0.5	50	400	23.0		
	10.0	50	309	23.0	HS/1500	
	5.0	50	346	21.0		
	0.5	50	450	22.0		
Morganite Modmor Inc. (1972)	5.0	173	238	21.8	Type IS (HM)	[268]
	0.5	136	324	18.0		
	0.2	120	352	19.1		
	0.1	86	371	16.1		
	5.0	206	334	22.9	Type IIS (HS)	
	0.5	136	444	18.3		
	0.2	133	480	20.3		
	0.1	123	494	16.9		
Commercial C-fibres (1974)	3.0 in.	–	215	27.0	GY-70, HM Celanese	[269]
	1.0 in.	–	240	25.0		
	0.25 in.	–	310	23.0		
	3.0 in.	–	363	20.0	Type-AS, HS Hercules	
	1.0 in.	–	441	20.0		
	0.25 in.	–	549	18.0		
	0.1 in.	–	636	11.0		
	3.0 in.	–	311	22.0	Thornel 300 Union-Carb.	
	1.0 in.	–	392	27.0		
	0.25 in.	–	482	18.0		
	0.1 in.	–	488	23.0		
Courtaulds (1979)	5.0 in.	24	359	17.4	Type HMS	
	0.5	10	428	24.0		
	0.05	10	550	15.7		
	5.0	25	400	13.4	Type HTS	
	0.5	10	528	14.4		
	0.25	10	503	25.3		

*10^3 psi ≡ 6.89 N mm^{-2}.

5.7. Variations with gauge length and fibre diameter

In addition to direct observations of defects by optical and electron microscopy, other experimental observations, e.g. variation of average tensile strength with fibre diameter and gauge length, also point to the importance of defects in the tensile failure of various carbon fibres. Moreton [266] measured the breaking strengths of carbon fibres heat treated over a range of temperatures between 1000 and 3000° C using gauge lengths of 0.5, 5 and 10 cm. Some typical results are included in Table IV, along with the results obtained by others. The average tensile strength values were found to decrease exponentially with increase in the gauge length. Detailed histograms also showed that the range of the strengths was displaced downward by the use of longer gauge lengths. The actual distribution of strengths was ascribed to the presence of randomly occurring defects. Comparison was therefore made with the weak-link theory of Tippett [267] and a reasonable correspondance was observed. Barry [268] has reported single filament testing of Modmor fibres, manufactured in early 1972 measured at four different gauge lengths (see Table V). A logarithmic plot of breaking strength against gauge length suggested a linear relationship. McMahon [269] extrapolated the tensile strength data from a similar study on various commercial fibres to a gauge length of 0.025 in. and used it to predict the tensile strength of undirectional composites through an empirical relationship. Hitchon and Phillips [270] measured breaking strengths of Courtaulds HMS and HTS fibres using gauge lengths of 0.05, 0.5 and 5 cm and observed that the strengths at shorter lengths were less than predicted from the 5 cm strength using the Weibull theory [271]. They explained it in terms of a bimodal or a combination of two unimodal flaw size distributions instead of a homogeneous unimodal distribution required by the Weibull theory. Two recent papers by Beetz [272, 273] also describe a bimodal distribution of strength in Thornel-P fibres. He has extended the Weibull theory to include a bimodal distribution which allowed more accurate estimates of mean fibre strength at short gauge lengths.

The effect of fibre diameter on the tensile properties of carbon fibre was studied by Lamotte and Perry [274, 275], Diefendorf *et al.* [276] and by Jones and Duncan [277]. Lamotte and Perry found that the strength of Grafil-HT fibres diminished by about 20% as their diameter rose from 7 to 12 μm, whereas the modulus decreased from 290 GPa at 7.5 μm to 250 GPa at 10.5 μm. Grafil-A fibres, which represent the intermediate product (starting from PAN) from which type HT fibres are made by a thermal treatment, did not show any dependence on fibre diameter. They have associated the decrease in tensile strength and modulus to a non-typical outer surface layer in thick fibres. Since different diameters are a result of different degrees of stretching of the precursor filaments in a tow during their manufacture or during their conversion to carbon fibres, an additional contribution could be from the different orientations, higher in smaller diameter fibres, introduced during these processes. A similar decrease in tensile strength and modulus was observed by Jones and Duncan [277] in experimental PAN-based carbon fibres. They attribute the variations in Young's modulus to the differences in the relative amounts of sheath and core structures in fibres of different diameters. According to them, thin fibres would possess a thicker sheath which shows better basal plane alignment than the core, while a thick fibre would contain a larger fraction of the core. The variations in the breaking strengths have been explained by them in terms of basal plane cracks which result from the anisotropic thermal contraction of the crystallites. More cracks are likely to occur in a thick fibre due to a larger core which would decrease the tensile strength of these fibres.

6. Modification of carbon fibre surface

The outstanding mechanical properties of carbon fibres become of practical interest only if they can be efficiently translated into a usable structural form such as composites, the properties of which depend to a large extent on the interaction between the fibre and the matrix. Composite characteristics which are highly dependent on fibre–resin coupling include flexural and interlaminar shear strength and modes of failure. Early work with carbon fibre–epoxy composites gave disappointingly low values for the interlaminar shear strength, a general measure of the adhesion at the interface. A considerable effort was subsequently devoted to the study of surface properties of carbon fibres [15, 25, 278–284] and possible alteration of the surface [279, 281, 285–288] for good fibre–matrix adhesion. Numerous procedures for altering the carbon fibre surface have been described in the open as well as patented literature. It is beyond the scope of this review to go into the details of these methods. The basis appears to be to change the chemical nature of the surface and to change the smooth surface of high strength and high modulus carbon fibres to a rough or porous surface, through a mild oxidation. Controlled oxidation has been successfully achieved by using both liquid [287, 289–291] and gaseous [292–295] oxidizing agents.

7. Concluding remarks

The structure and properties of carbon fibres depend, in addition to the precursor properties, on the stabilization and carbonization conditions employed during their manufacture. The morphology of the precursor fibres plays an important role. The importance of proper optimization and control of stabilization and carbonization during the conversion of PAN-based precursor fibres to carbon fibres is quite evident from the literature reviewed here. This requires the use of suitable techniques for characterizing the fibre at various stages during these operations. It is clear from published literature that the constraints imposed on many precursor fibres during stabilization and/or carbonization play an important role. The techniques or measurements which are sensitive to the differences in the fibre structure and properties during their heat treatment with different levels of constraints therefore become important.

The morphological order developed during spinning and drawing operations could be considerably different depending on the conditions employed during these processes. These precursors with different morphologies could require, in spite of their same chemical composition and denier/filament, quite different stabilization and carbonization conditions in order to produce carbon fibres with good mechanical properties. This emphasizes the need for studies of initial morphology and the changes in it as a function of the progression of stabilization and carbonization in precursor fibres with significantly different orientations and other morphological parameters.

There is indeed a vast amount of literature on the conversion of acrylonitrile-based precursors to carbon fibres. Much of it, unfortunately, is on isolated aspects of this complex process and so fails to provide a cohesive link between the various material and process aspects. A high degree of empiricism exists still in determining the optimum conditions of processing. It is necessary to conduct comprehensive research on the chemical and morphological aspects of the conversion of precursor polymer to carbon fibres in order to improve our understanding of the evolution of structure and properties of these critical high performance materials. Many successful processes have indeed been designed with only a partial understanding of fundamental aspects. It is our belief, nevertheless, that these can be significantly improved and that new processes for new precursor compositions can be designed with greater ease through improved comprehension at an elementary level.

Acknowledgements

The authors express their appreciation to Mr Prashant Desai and Dr M. Balasubramanian for the numerous ways in which they helped in the preparation of this review. Financial support from the Office of Naval Research for this study is gratefully acknowledged. The authors express their deep gratitude to Dr L. H. Peebles for many valuable suggestions regarding this study.

References

1. R. BACON, *J. Appl. Phys.* **31** (1960) 283.
2. Union Carbide Corp., USA US Patent 2957756 (1960).
3. *Idem*, US Patent 3454362 (1969).
4. *Idem*, US Patent 3503708 (1970).
5. A. SHINDO, *Osaka Kogyo Gijitsu Shikuko Kiko* **12** (1961) 110.
6. *Idem, ibid.* **12** (1961) 119.
7. *Idem, Rep. Gov. Ind. Res. Inst. Osaka* No. 317 (1961).
8. *Idem, Carbon* **1** (1964) 391.
9. W. JOHNSON, L. PHILLIPS and W. WATT, US Patent 3412062 (1968).
10. P. J. GOODHEW, A. J. CLARKE and J. E. BAILEY, *Mater. Sci. Eng.* **17** (1975) 3.
11. D. H. LOGSDAIL, *Appl. Polym. Symp.* **9** (1969) 245.
12. W. WATT, *Carbon* **10** (1972) 121.

13. D. J. JOHNSON, in Proceedings of the 61st Annual Conference (Manchester, Textile Institute, 1977) p. 73.
14. P. E. MORGAN, *Textile Prog.* **8** (1976) 69.
15. D. W. McKEE and V. J. MIMEAULT, "Chemistry and Physics of Carbon", Vol. 8, edited by P. A. Thrower and P. L. Walker (Dekker, New York, 1973) p. 151.
16. R. BACON, *Appl. Polym. Symp.* **9** (1969) 213.
17. P. G. ROSE, PhD thesis, University of Aston, UK (1971).
18. C. W. LeMAISTRE, PhD thesis, Rennslaer Polytechnic Institute, New York (1972).
19. P. W. BARRY, PhD thesis, University of Newcastle, Australia (1974).
20. R. MORETON, PhD thesis, University of Surrey UK (1976).
21. S. B. WARNER, ScD thesis, Massachussetts Institute of Technology, USA (1976).
22. O. ZUBZANDA, PhD thesis, University of New South Wales, Australia (1980).
23. Th. MUELLER, PhD thesis, University of Karlsruhe, FRG (1982).
24. M. K. JAIN, PhD thesis, Georgia Institute of Technology, Atlanta, Georgia, USA (1984).
25. H. H. GIBBS, R. C. WENDT and F. C. WILSON, *Polym. Eng. Sci.* **19** (1979) 342.
26. B. H. ECKSTEIN, *Fibre Sci. Technol.* **14** (1981) 139.
27. J. WARD, private communication, American Cyanamid, USA (1983).
28. L. M. MANOCHA and O. P. BHAL, *Die Angew. Makromol. Chemie* **64** (1977) 115.
29. E. V. THOMPSON, *J. Polym. Sci. Polym. Lett.* **4** (1966) 361.
30. W. N. TURNER and F. C. JOHNSON, *J. Appl. Polym. Sci.* **13** (1969) 2073.
31. J. W. JOHNSON, P. G. ROSE and G. SCOTT, in Proceedings of the 3rd Conference on Industrial Carbon and Graphite, London (Soc. Chem. Ind., London, 1970) p. 443.
32. Toray Industries Inc., US Patent 4065549 (1977).
33. W. WATT and W. JOHNSON, in Proceedings of the 3rd Conference on Industrial Carbon and Graphite, London (Soc. Chem. Ind., London, 1970) p. 417.
34. W. WATT, D. J. JOHNSON and E. PARKER, in Proceedings of the Plastics and Polymers Conference, Suppl. **6** (Plastics Institute, London, 1974) 3.
35. Great Lakes Carbon Corp., New York, US Patent 3533743 (1970).
36. O. P. BAHL and L. M. MANOCHA, *Die Angew. Makromol. Chemie* **48** (1975) 145.
37. L. M. MANOCHA, O. P. BAHL and G. C. JAIN, *ibid.* **67** (1978) 11.
38. O. P. BAHL and L. M. MANOCHA, *Fibre Sci. Technol.* **9** (1976) 77.
39. *Idem, Carbon* **13** (1975) 297.
40. S. P. VARMA, B. B. LAL and N. K. SRIVATSAVA, *ibid.* **14** (1976) 207.
41. J. E. BAILEY and A. J. CLARKE, *Nature* **234** (1971) 529.
42. J. SIMITZIS, *J. Coll. Polym. Sci.* **255** (1977) 1074.
43. J. FERGUSON and N. DEBNATH-RAY, *Fibre Sci. Technol.* **13** (1980) 167.
44. L. I. KOMLYAKOVA, N. V. PISKAREV, N. V. BALYEV, V. A. MIKHAILOVA and N. V. POLYAKOVA, *Khim. Volokna* **2** (1976) 49.
45. M. M. COLEMAN and R. J. PETCAVICH, *J. Polym. Sci. Polym. Phys. Ed.* **16** (1978) 821.
46. M. M. COLEMAN and G. T. SIVY, *Carbon* **19** (1981) 123.
47. *Idem, ibid.* **19** (1981) 127.
48. *Idem, ibid.* **19** (1981) 133.
49. M. M. COLEMAN, G. T. SIVY, P. C. PAINTER, R. W. SNYDER and B. GORDON III, *ibid.* **21** (1983) 255.
50. L. E. WOLFRAM, J. G. GRASSELLI and J. L. KOENIG, *Appl. Polym. Symp.* (1974) 25.
51. *Idem, ibid.* (1974) 27.
52. R. T. CONLEY and J. F. BIERON, *J. Appl. Polym. Sci.* **7** (1963) 1757.
53. I. NOB and H. YU, *J. Polym. Sci. Polym. Lett.* **B4** (1966) 721.
54. W. J. BURLANT and J. L. PARSONS, *J. Polym. Sci.* **22** (1956) 249.
55. W. WATT, in Proceedings of the 3rd Conference on Industrial Carbon and Graphite, London (Soc. Chem. Ind., London, 1970) p. 431.
56. G. RADHAKRISHNAN, T. NAGABHUSHANAM, K. J. JOSEPH and M. SANTHAPPA, *Makromol. Chem.* **180** (1979) 2923.
57. J. BROMLEY, in Proceedings of the International Conference on Carbon Fibres, their Composites and Applications, Plastic Institute, London (1971) p. 3.
58. M. MINAGAWA and T. IWAMATSU, *J. Polym. Sci. Polym. Chem. Ed.* **18** (1980) 481.
59. E. FITZER and D. J. MULLER, *ACS Polym. Chem. Symp.* (1973) 396.
60. *Idem, Carbon* **13** (1975) 63.
61. Y. N. SAZANOV, N. A. SHIROKOV and B. E. GOLTSIN, *Thermo Chimica Acta* **32** (1979) 73.
62. C. A. GAULIN and W. R. McDONALD, Air Force Report SAMSO-TR-71-61 I (1971).
63. A. GUYOT and M. BERT, *Eur. Polym. J.* **14** (1978) 101.
64. J. SIMITZIS, *Coll. Polym. Sci.* **255** (1977) 948.
65. E. URBAS and E. KULLIK, *J. Chromatography* **137** (1977) 210.
66. Y. TSUCHIYA and K. SUMI, *J. Appl. Polym. Sci.* **21** (1977) 975.
67. S. SATONAKA and J. MATSUI, *Plastics Industry News* **26** (1980) 151.
68. E. I. KAZAKOV, M. A. KOSTAMAROVA, Z. S. SMUTKINA, M. E. KAZAKOV, N. F. KARPOVA, V. I. KASATOCHKIN and N. P. RADIMOV, *Khim Volokna* **6** (1971) 27.
69. R. S. LEHRLE, J. C. ROBB and J. R. SUGGATE, *Eur. Polym. J.* **18** (1982) 443.
70. W. WATT and J. GREEN, in Proceedings of the International Conference on Carbon Fibres, their Composites and Applications (Plastics Institute, London, 1971) p. 23.
71. C. A. GAULIN and W. R. McDONALD, Air Force Report SAMSO-TR-72-304 II (1972).
72. S. S. CHEN, J. HERMS, L. H. PEEBLES Jr and D. R. UHLMANN, *J. Mater. Sci.* **16** (1981) 1490.
73. G. AYREY, S. K. CHADDA and R. C. POLLER, *Eur. Polym. J.* **19** (1983) 313.
74. J. N. HAY, *J. Polym. Sci. A-1* **6** (1968) 2127.
75. N. GRASSIE, "Developments in Polymer Degradation" (Applied Science, London, 1977) p. 133.
76. N. GRASSIE and R. McGUCHAN, *Eur. Polym. J.* **6** (1970) 1277.
77. *Idem, ibid.* **7** (1971) 1091.
78. *Idem, ibid.* **7** (1971) 1357.
79. *Idem, ibid.* **7** (1971) 1503.
80. *Idem, ibid.* **8** (1972) 243.
81. *Idem, ibid.* **8** (1972) 257.
82. *Idem, ibid.* **8** (1972) 865.
83. H. H. G. JELLINEK and A. DAS, *J. Polym. Sci. Polym. Chem. Ed.* **16** (1978) 2715.
84. M. M. KANOVICH and A. P. RUDENKO, *Khim. Volokna* **3** (1982) 19.
85. J. W. JOHNSON, W. D. POTTER, P. G. ROSE and G. SCOTT, *Br. Polym. J.* **4** (1972) 527.
86. A. J. CLARKE and J. E. BAILEY, *Nature* **243** (1973) 146.
87. W. D. POTTER and G. SCOTT, *Nature Phys. Sci.* **236** (1972) 30.
88. L. H. PEEBLES Jr, *J. Polym. Sci. A-1* **5** (1967) 2637.
89. L. H. PEEBLES Jr and J. BRANDRUP, *Makromol. Chem.* **98** (1966) 189.
90. L. H. PEEBLES Jr, "Encyclopedia of Chemical Technology, Suppl"., (Wiley, New York, 1979) p. 1.
91. G. M. KERCH, A. M. TOLKS, G. A. KARLSON and L. A. IRGEM, *Khim Volokna* **2** (1978) 50.
92. R. C. ROWE, NTIS Report, AD-755427 (National

Technical Information Service, Springfield, Virginia, 1972).

93. Toho Beslon Co Ltd, US Patent 4 069 297 (1978).
94. National Research and Development Council, UK, US Patent 4 079 122 (1978).
95. Japan Exlan Co Ltd, US Patent 4 009 991 (1977).
96. W. WATT and W. JOHNSON, *Nature* **257** (1975) 210.
97. S. B. DARNER, L. H. PEEBLES Jr and D. R. UHLMANN, *J. Mater. Sci.* **14** (1979) 556.
98. J. S. PERKINS, R. J. SACHER, R. J. SHUFORD, G. R. THOMAS and S. E. WENTWORTH, NTIS Report AD-750362 (National Technical Information Service, Springfield, Virginia, 1972).
99. G. K. LAYDEN, *Carbon* **10** (1972) 59.
100. B. DANNER and J. MEYBECH, in Proceedings of the International Conference on Carbon Fibres, their Composites and Applications (Plastics Institute, London, 1971) p. 36.
101. M. V. G. I. STANCHENKO, M. V. ABRAMOV, B. P. MORIN and M. V. SHABLYGIN, *Khim. Volokna* **1** (1981) 20.
102. D. BRAUN and R. DISSELHOFF, *Die Angew. Makromol. Chemie* **74** (1978) 225.
103. E. FITZER and A. K. FIELDER, *ACS Polym. Chem. Symp.* **14** (1973) 401.
104. V. C. McLOUGHLIN and R. MORETON, NTIS Report AD-A026-743 (National Technical Information Service, Springfield, Virginia, 1974).
105. Japan Exlan Co Ltd, British Patent 1 500 675 (1978).
106. *Idem*, US Patent 4 154 807 (1979).
107. Celanese Corp., New York, US Patent 4 002 426 (1977).
108. D. E. CAGLIOSTRO, *Text. Res. J.* **50** (1980) 632.
109. I. L. KALNIN, A. H. DiEDWARDO, E. W. CHOE and J. M. RHODES, *Org. Coat. Plast. Chem.* **38** (1978) 685.
110. Monsanto Co., St. Louis, US Patent 3 814 577, (1974).
111. Celanese Corp., New York, US Patent 4 004 053 (1977).
112. *Idem*, US Patent 4 364 916 (1982).
113. *Idem*, US Patent 3 850 876 (1974).
114. Great Lakes Carbon Corp., New York, US Patent 4 279 612 (1981).
115. A. H. DiEDWARDO, *Org. Coat. Plast. Chem.* **38** (1978) 692.
116. K. MORITA, H. MIYACHI and T. HIRAMTSU, *Carbon* **19** (1981) 11.
117. O. P. BAHL, R. B. MATHUR and K. D. KUNDRA, *Fibre Sci. Technol.* **13** (1980) 155.
118. Nippon Carbon Co., Japan, US Patent 3 529 934 (1970).
119. J. W. JOHNSON, *Appl. Polym. Symp.* **9** (1969) 229.
120. G. A. COOPER and R. M. MAYER, *J. Mater. Sci.* **6** (1971) 60.
121. R. MORETON, W. WATT and W. JOHNSON, *Nature* **213** (1967) 690.
122. D. A. BRANDRETH, W. M. RIGGS and R. E. JOHNSON, *Nature Phys. Sci.* **236** (1972) 10.
123. Toho Beslon Co Ltd, Japan US Patent 4 073 870 (1978).
124. H. B. EZEKIEL, US Patent 3 635 675 (1972).
125. *Idem*, US Patent 3 671 192 (1972).
126. *Idem, Appl. Polym. Symp.* **21** (1973) 167.
127. *Idem, ibid.* **21** (1973) 153.
128. J. W. JOHNSON, J. R. MARJORAM and P. G. ROSE, *Nature* **221** (1969) 357.
129. W. JOHNSON, in Proceedings of the 3rd Conference on Industrial Carbon and Graphite, London (Soc. Chem. Ind., London, 1970) p. 447.
130. Union Carbide Corp., USA, US Patent 3 454 362 (1969).
131. Ames Research Center, California, NASA Tech. Briefs, Spring (1983).
132. Celanese Corp., USA, US Patent 3 723 605 (1973).
133. V. DIETZ, US Patent 3 931 392 (1976).
134. W. WATT and W. JOHNSON, *Appl. Polym. Symp.* **9** (1969) 215.
135. D. J. MULLER, E. FITZER and A. K. FIEDLER, in Proceedings of the International Conference on Carbon Fibres, their Composites and Applications (Plastics Institute, London, 1971) paper 2.
136. E. FITZER and D. J. MULLER, *Die Makromol. Chemie* **144** (1971) 117.
137. E. FITZER and M. HEYM, *Chem. Ind.* **16** (1976) 663.
138. G. IK. LAYDEN, *J. Appl. Polym. Sci.* **15** (1971) 1709.
139. O. P. BAHL and R. B. MATHUR, *Fibre Sci. Technol.* **12** (1979) 31.
140. E. FITZER and M. HEINE, in Proceedings of the 16th Biennial Conference on Carbon, San Diego, California 1983 (American Carbon Society, 1983) p. 501.
141. S. B. WARNER, L. H. PEEBLES Jr and D. R. UHLMANN, *J. Mater. Sci.* **14** (1979) 565.
142. A. TAKAKU, S. TERUI, C. SUZUKI and J. SHIMIZU, *Fibre Sci. Technol.* **16** (1981) 237.
143. A. TAKAKU, S. KOBAYASHI, *et al.*, *ibid.* **15** (1981) 87.
144. V. G. HINRICHSEN and H. ORTH, *Kolloid Z. Z. Polymere* **247** (1971) 844.
145. L. G. WALLNER and K. RIGGERT, *J. Polym. Sci. Polym. Lett.* **1** (1963) 111.
146. P. H. LINDENMEYER and R. HOSEMANN, *J. Appl. Phys.* **34** (1963) 42.
147. R. STEFANI, M. CHEVRETON, M. GARNIER and M. C. EYRAUD, *Acad. des Sciences* (1960) 2147.
148. *Idem, ibid.* (1959) 2006.
149. B. G. COLVIN and P. STORR, *Eur. Polym. J.* **10** (1974) 337.
150. A. K. GUPTA and N. CHAND, *ibid.* **15** (1979) 899.
151. R. B. BEEVERS, E. F. WHITE and L. BROWN, *Farad. Trans.* (1960) 1535.
152. Y. IMAI, S. MINAMI, T. YOSHIHARA, Y. JOH and H. SATO, *J. Polym. Sci. Polym. Lett.* **8** (1970) 281.
153. F. KUMAMARU, T. KAJIYAMA and M. TAKAYANAGI, *J. Crystal Growth* **48** (1980) 202.
154. V. F. HOLLAND, S. B. MITCHELL, W. L. HUNTER and P. H. LINDENMEYER, *J. Polym. Sci.* **62** (1962) 145.
155. J. J. KLEMENT and P. H. GEIL, *ibid. A2* **6** (1968) 1381.
156. C. R. BOHN, J. R. SCHAEFGEN and W. O. STATTON, *ibid.* **55** (1961) 531.
157. R. C. HOUTZ, *Text. Res. J.* (1950) 786.
158. S. B. WARNER, D. R. UHLMANN and L. H. PEEBLES Jr, *J. Mater. Sci.* **14** (1979) 1893.
159. H. A. STUART, *Physik der Hochpolymeren* **3** (1955) 167.
160. G. HINRICHSEN and H. ORTH, *J. Polym. Sci. Polym. Lett.* **9** (1971) 529.
161. R. B. HURLEY and L. S. TZENTIS, *ibid.* **1** (1963) 423.
162. M. TAKAHASHI and Y. NUKUSHINA, *J. Polym. Sci. S19* **163** (1962) 56.
163. V. F. HOLLAND, *ibid.* **142** (1960) 572.
164. R. M. GOHIL, K. C. PATEL and R. D. PATEL, *Die Angew. Makromol. Chemie* **25** (1972) 83.
165. J. P. CRAIG, J. P. KNUDSEN and V. F. HOLLAND, *Text. Res. J.* **32** (1962) 435.
166. P. TUCKER and W. GEORGE, *Polym. Eng. Sci.* **12** (1972) 364.
167. G. NATTA and G. DALL'ASTA, Italian Patent 570 434 (1959).
168. G. H. OLIVE and S. OLIVE, *Adv. Polym. Sci.* **32** (1979) 123.
169. J. L. KOENIG, L. E. WOLFRAM and J. G. GRASSELLI, *J. Macromol. Sci. Phys. Ed. B4* **3** (1970) 491.
170. I. M. FOUDA and K. A. ELFARHATY, *Acta Physica Polonica* **A61** (1982) 137.
171. I. B. KLIMENKO and L. V. SMIRNOV, *Vsokomol. Soyed.* **5** (1963) 1520.
172. R. CHIANG, *J. Polym. Sci.* **A1** (1963) 2765.
173. W. R. KRIGBAUM and N. TOKITA, *ibid.* **XLIII** (1960) 467.
174. B. G. FRUSHOUR, *Polym. Bull.* **4** (1981) 305.
175. *Idem, ibid.* **7** (1982) 1.
176. D. J. THORNE and J. R. MARJORAM, *J. Appl. Polym. Sci.* **16** (1972) 1357.
177. L. E. ALEXANDER, "X-Ray Diffraction Methods in Polymer Science", (Wiley, New York, 1969).
178. M. E. FILLERY and P. J. GOODHEW, *Nature Phys. Sci.* **233** (1971) 118.
179. C. N. TYSON, *ibid.* **229** (1971) 121.
180. G. HINRICHSEN, *J. Appl. Polym. Sci.* **17** (1973) 3305.

181. S. B. WARNER, *J. Polym. Sci. Polym. Lett. Ed.* **16** (1978) 287.
182. L. E. ALEXANDER, "X-ray Diffraction Methods in Polymer Science", (Wiley, New York, 1969) p. 423.
183. D. J. JOHNSON, Extended Abstracts of the 15th Biennial Conference on Carbon, Philadelphia (American Carbon Society, 1981) p. 304.
184. W. RULAND and H. TOMPA, *Acta. Crystallogr.* **A24** (1968) 93.
185. *Idem, J. Appl. Cryst.* **5** (1972) 225.
186. W. RULAND, *J. Appl. Phys.* **38** (1967) 3585.
187. V. I. KASATOCHKIN, Z. S. SMUTKINA, M. A. KAZAKOV, M. A. CHUBAROVA and N. P. RADIMOV, *Khim Volokna* **4** (1972) 10.
188. D. J. JOHNSON, *Phil. Trans. R. Soc. Lond.* **A294** (1980) 443.
189. D. J. JOHNSON, in Proceedings of the International Conference on Carbon Fibres, their Composites and Applications, Vol. 4 (Plastics Institute, London, 1971) paper 8.
190. L. FISCHER and W. RULAND, *Coll. Polym. Sci.* **258** (1980) 917.
191. W. RULAND, *Appl. Polym. Symp.* **9** (1969) 293.
192. R. J. DIEFENDORF and E. TOKARSKY, *Polym. Eng. Sci.* **15** (1975) 150.
193. S. C. BENNETT and D. J. JOHNSON, *Carbon* **17** (1979) 25.
194. *Idem*, in Proceedings of the Fifth International Conference on Carbon and Graphite, London (Soc. Chem. Ind., London, 1978) p. 377.
195. D. J. JOHNSON, D. CRAWFORD and B. F. JONES, *J. Mater. Sci.* **8** (1973) 286.
196. B. J. WICKS, *ibid.* **6** (1971) 173.
197. B. J. WICKS and R. A. COYLE, *ibid.* **11** (1976) 376.
198. D. J. JOHNSON and C. N. TYSON, *Brit. J. Appl. Phys. J. Phys. D* **2** (1969) 787.
199. R. PERRET and W. RULAND, *J. Appl. Cryst.* **3** (1970) 525.
200. D. J. JOHNSON and C. N. TYSON, *J. Phys. D Appl. Phys.* **3** (1970) 527.
201. R. PERRET and W. RULAND, *J. Appl. Cryst.* **2** (1969) 209.
202. P. DEBYE and A. M. BEUCHE, *J. Appl. Phys.* **20** (1949) 1518.
203. G. POROD, *Kolloidzeit* **124** (1951) 83.
204. *Idem, ibid.* **125** (1951) 51, 108.
205. P. DEBYE, H. R. ANDERSON and H. BRUMBERGER, *J. Appl. Phys.* **28** (1957) 679.
206. W. JOHNSON and W. WATT, *Nature* **215** (1967) 384.
207. D. V. BADAMI, J. C. JOINER and G. A. JONES, *ibid.* **215** (1967) 387.
208. B. J. WICKS, *J. Mater. Sci.* **6** (1971) 173.
209. W. RULAND, *Polym. Preprints* **9** (1968) 1368.
210. D. H. SPENCER, M. A. HOOKER, A. C. THOMAS and B. A. NAPIER, in Proceedings of the International Carbon Conference, London (Soc. Chem. Ind., London, 1970) p. 467.
211. J. B. JONES and L. S. SINGER, *Carbon* **20** (1982) 379.
212. D. ROBSON, F. Y. I. ASSABGHY, D. J. E. INGRAM and P. G. ROSE, in Proceedings of the 3rd Conference on Industrial Carbon and Graphite, London (Soc. Chem. Ind., London, 1970) p. 453.
213. D. H. SAUNDERSON and C. G. WINDSOR, *ibid.*, p. 438.
214. C. W. LeMAISTRE and R. J. DIEFENDORF, *SAMPE Q.* **4**(4) (1973) 1.
215. R. H. KNIBBS, *J. Microscopy* **94** (1971) 273.
216. C. W. LeMAISTRE and R. J. DIEFENDORF, Proceedings of the Advances in Material Composites and Carbon, Symposia of the American Ceramic Society (American Ceramic Society, Columbus, Ohio, 1972) p. 77.
217. J. A. GRIFFOTHS and H. MARSH, Extended Abstracts of the 12th Biennial Conference on Carbon (American Carbon Society, St Marys, Pennsylvania, 1981) p. 316.
218. P. KWIZERA, M. S. DRESSELHAUS, D. R. UHLMANN, J. S. PERKINS and C. R. DESPER, *Carbon* **20** (1982) 387.
219. F. R. BARNET and M. K. NORR, *ibid.* **11** (1973) 281.
220. *Idem*, in Proceedings of the International Conference on Carbon Fibres, their Composites and Applications (Plastics Institute, London, 1974) p. 32.
221. W. JOHNSON, *Nature* **279** (1979) 142.
222. D. CRAWFORD and D. J. JOHNSON, *J. Micros.* **94** (1971) 51.
223. J. A. HUGO, V. A. PHILLOPS and B. W. ROBERTS, *Nature* **226** (1970) 144.
224. W. RULAND, *ACS Polym. Preprints* **9** (1968) 1368.
225. A. OBERLIN, F. MOLLEYRE and M. BASTICK, Extended Abstracts of the 13th Biennial Conference on Carbon (American Carbon Society, St Marys, Pennsylvania, 1977) p. 371.
226. R. BACON and A. F. SILVAGGI, *Carbon* **9** (1971) 321.
227. Z. MENCIK, H. K. PLUMMER Jr and L. BARTOSIEWICZ, *ibid.* **13** (1975) 417.
228. E. FITZER and J. SIMITZIS, Extended Abstracts of the 12th Biennial Conference on Carbon (American Carbon Society, St Marys, Pennsylvania, 1975) p. 291.
229. ASTM D 3039-76, "Annual Book of ASTM Standards", Vol. **36** (1978) 721.
230. P. E. McMAHON, in Proceedings of the Symposium by ASTM D30 Committee, STP-521 (1973) 367.
231. Rolls-Royce Ltd, French Patent 1 590 257 (1970).
232. W. N. REYNOLDS, in Proceedings of the 3rd Conference on Industrial Carbon and Graphite, London (1970) p. 472.
233. S. ROSENBAUM, *J. Appl. Polym. Sci.* **9** (1965) 2071.
234. O. P. BAHL and L. M. MANOCHA, *Carbon* **12** (1974) 417.
235. J. FERGUSON and B. MAHAPATRO, *Fibre Sci. Technol.* **9** (1976) 161.
236. *Idem, ibid.* **11** (1978) 55.
237. S. D. FEDOSEEV, T. V. KOMAROVA and A. K. ZAKHAROV, *Khim. Volokna* **6** (1976) 24.
238. W. N. REYNOLDS and R. MORETON, *Phil. Trans. R. Soc. Lond.* **A294** (1980) 451.
239. R. MORETON and W. WATT, *Carbon* **12** (1974) 543.
240. R. MORETON, in Proceedings of the 3rd Conference on Industrial Carbon and Graphite, London (Society of Chemical Industries, London, 1970) p. 472.
241. *Idem*, in Proceedings of the International Conference on Carbon Fibres, their Composites and Applications, Plastic Institute, London, (1971) paper 12.
242. T. ISHIKAWA, R. MAKI and M. MORISHITA, in Proceedings of the ACS 161st National Meeting, Los Angeles (ACS, Washington, DC, 1971) p. 400.
243. *Idem*, ACS 161st National Meeting, Division of Cellulose Wood and Fibre Chemistry (ACS, Washington, DC, 1971) paper 26.
244. E. FITZER and T. MULLER, Extended Abstracts of the 15th Biennial Conference on Carbon (1981) p. 312.
245. G. RADHAKRISHNAN, K. T. JODHEP and M. SANTAPPA, *Leather Sci.* **28** (American Carbon Society, St Marys, Pennsylvania, 1981) p. 27.
246. T. NAGABHUSHANAM, Th. MULLER, A. E. SIMIONATA and J. L. GOMES DE SILVA, Extended Abstracts of the 16th Biennial Conference on Carbon (American Carbon Society, St Marys, Pennsylvania, 1983) p. 509.
247. E. FITZER and J. SIMITZIS, Extended Abstracts of the 12th Biennial Conference on Carbon (American Carbon Society, St Marys, Pennsylvania, 1983) p. 291.
248. National Research and Development Council, UK, Canadian Patent 1 132 297 (1982).
249. D. GOLDEN and P. ROSE, in Proceedings of the 5th International Conference on Carbon and Graphite, London (American Carbon Society, St Marys, Pennsylvania, 1978) p. 388.
250. S. S. CHARI, O. P. BAHL and R. B. MATHUR, *Fibre Sci. Technol.* **15** (1981) 153.
251. O. P. BAHL, R. B. MATHUR and K. D. KUNDRA, *ibid.* **15** (1981) 147.
252. J. P. KENNEDY and C. M. FONTANA, *J. Polym. Sci.*

39 (1959) 501.
253. V. O. GORBACHEVA and E. AV. KHLEBNIKOVA, *Khim. Volokna* **6** (1976) 42.
254. Y. KOBAYASHI, S. OKAJIMA and H. KOSUDA, *J. Appl. Polym. Sci.* **11** (1967) 2525.
255. F. J. DIEFENDORF, *Div. Petroleum Chem. Preprints* **20** (1975) 447.
256. W. R. JONES and J. W. JOHNSON, *Carbon* **9** (1971) 645.
257. J. P. STERRY and W. L. LACHMAN, *Chem. Eng. Progr.* **58** (1962) 37.
258. W. N. REYNOLDS, "Chemistry and Physics of Carbon", edited by P. A. Thrower and P. L. Walker, Vol. **11** (1973) p. 1.
259. M. STEWART and M. FEUGHELMAN, *J. Mater. Sci.* **8** (1973) 1119.
260. S. C. BENNETT and D. J. JOHNSON, *ibid.* **18** (1983) 3337.
261. W. WATT and W. JOHNSON, in Proceedings of the 3rd Conference on Industrial Carbon and Graphite, London (Society of Chemical Industries, London, 1970) p. 417.
262. J. W. JOHNSON and D. J. THORNE, *Carbon* **7** (1969) 659.
263. D. J. THORNE, V. J. GOUGH and G. HIPKISS, *Fibre Sci. Technol.* **3** (1970) 119.
264. J. V. SHARP, S. G. BURNAY, J. R. MATHEWS and E. A. HARPER, in Proceedings of the International Conference on Carbon Fibres, their Composites and Applications (Plastics Institute, London, 1974) paper 5.
265. E. V. MURPHY and B. F. JONES, *Carbon* **9** (1971) 91.
266. R. MORETON, *Fibre Sci. Technol.* **1** (1968) 271.
267. L. H. C. TIPPETT, *Biometrika* **17** (1925) 364 (from [254]).
268. P. W. BARRY, *Fibre Sci. Technol.* **11** (1978) 245.
269. P. E. McMAHON, *SAMPE Q.* October (1974) 7.
270. J. W. HITCHON and D. C. PHILLIPS, *Fibre Sci. Technol.* **12** (1979) 217.
271. W. WEIBULL, *J. Appl. Mech.* **18** (1951) 293 (from [258]).
272. C. P. BEETZ Jr, *Fibre Sci. Technol.* **16** (1982) 45.
273. *Idem*, Extended Abstracts of the 15th Biennial Conference on Carbon (American Carbon Society, St Marys, Pennsylvania, 1981) p. 300.
274. A. J. PERRY, K. PHILLIPS and E. De LAMOTTE, *Fibre Sci. Technol.* **3** (1971) 317.
275. E. De LAMOTTE and A. J. PERRY, *ibid.* **3** (1970) 157.
276. R. J. DIEFENDORF, K. J. CHEN, W. P. SEAGROVES and J. J. -H. WANG, Tech. Report AD A096473 (Rensselaer Polytechnic Institute, Troy, New York, 1981).
277. B. F. JONES and R. G. DUNCAN, *J. Mater. Sci.* **6** (1971) 289.
278. P. BLESS and J. B. LANDO, *J. Polym. Sci. Polym. Lett.* **13** (1975) 153.
279. L. T. DRZAL, J. A. MESCHER and D. L. HALL, *Carbon* **17** (1979) 375.
280. J. B. DONNET and H. DAUKSCH, in Proceedings of the International Conference on Carbon Fibres, their Composites and Applications (Plastics Institute, London, 1971) paper 7.
281. B. RAND and R. ROBINSON, *Carbon* **15** (1977) 257.
282. F. HOPFGARTEN, *Fibre Sci. Technol.* **11** (1978) 67.
283. E. FITZER, K. H. GEIGL and L. M. MANOCHA, *Man Made Text. India* **21** (1978) 193.
284. O. P. BAHL and L. M. MANOCHA, *Die Angew. Makromol. Chemie* **75** (1979) 137.
285. J. H. CRANMER, G. C. TESORO and D. R. UHLMANN, *Ind. Eng. Chem. Prod. Res. Dev.* **21** (1982) 185.
286. E. FITZER, K. H. GEIGL and W. HUTTNER, *Carbon* **18** (1980) 265.
287. United Aircraft Corp., US Patent 3 660 140 (1972).
288. *Idem*, US Patent 3 720 536 (1973).
289. Union Carbide Corp., US Patent 3 791 840 (1974).
290. R. DAUKSYS, US Patent 3 801 350 (1974).
291. V. DIETZ, US Patent 3 931 392, (1976).
292. National Research and Development Council, UK, US Patent 3 476 703 (1969).
293. United Aircraft Corp., US Patent 3 720 536 (1973).
294. F. MOLLEYEYRE and M. BASTICK, in Proceedings of the International Conference on Carbon. BadHonnef, FRG. (1976) 500, from J. Delmonte, "Technology of Carbon and Graphite Fibre Composites" (Van Nostrand Reinhold, New York) p. 33.
295. L. P. KOBETS, N. V. POLYAKOVA, M. A. KUZETSOVA, O. B. KOLYASINSKAYA, V. S. SAMOILOV and N. V, BONDARENKO, *Polymer Mech.* **4** (1979) 4.

Received 8 October 1985
and accepted 22 May 1986